Copy
RM L52I03

NACA

RESEARCH MEMORANDUM

THRUST LOADING OF THE NACA 3-(3)(05)-05 EIGHT-BLADE DUAL-ROTATING PROPELLER AS DETERMINED FROM WAKE SURVEYS

By Robert J. Platt, Jr.

Langley Aeronautical Laboratory
Langley Field, Va.

NATIONAL ADVISORY COMMITTEE
FOR AERONAUTICS

WASHINGTON

October 30, 1952

NACA RM L52I03

NATIONAL ADVISORY COMMITTEE FOR AERONAUTICS

RESEARCH MEMORANDUM

THRUST LOADING OF THE NACA 3-(3)(05)-05 EIGHT-BLADE DUAL-ROTATING PROPELLER AS DETERMINED FROM WAKE SURVEYS

By Robert J. Platt, Jr.

SUMMARY

Wake-survey measurements of the thrust loading of the NACA 3-(3)(05)-05 eight-blade dual-rotating propeller are presented to supplement the previously published force-test results for this propeller. The data are presented for blade angles of 65°, 70°, 75°, and 80°, measured at 0.75R, at forward Mach numbers from 0.35 to 0.925.

The results indicate that changes in the lift-curve slopes of the airfoil sections have a secondary influence in producing the large decreases in thrust loading which occur at high Mach numbers. These decreases in thrust are primarily the result of changes in the angles of zero lift and increases in the drag coefficients of the airfoil sections. The changes in thrust loading with Mach number were found to be less pronounced at the tip sections than at the inboard sections.

INTRODUCTION

The results of force-test measurements of thrust, power, and efficiency for the NACA 3-(3)(05)-05 eight-blade dual-rotating propeller at forward Mach numbers to 0.925 were presented in reference 1. To supplement these data, surveys of total pressure in the propeller wake were made simultaneously with the force measurements. These pressure data have been reduced to section thrust coefficients which are presented herein to indicate some of the effects of Mach number on the thrust loading of a dual-rotating propeller.

SYMBOLS

b	blade width (chord)
C_T	thrust coefficient, $\frac{T}{\rho n_F^2 D^4}$
$\frac{dC_T}{dx_w}$	section thrust coefficient, $\frac{dT}{dx_w}\frac{1}{\rho n_F^2 D^4}$
D	propeller diameter
h	blade section maximum thickness
J	advance ratio, $\frac{V_o}{nD}$
M	Mach number of advance (tunnel Mach number uncorrected for tunnel-wall constraint)
n	propeller rotational speed, rps
R	propeller-tip radius
r	radius to a blade element
r_w	radius to a wake station
T	thrust
V_o	equivalent free-air velocity of advance (tunnel velocity corrected for tunnel-wall constraint)
x	blade-element station, $\frac{r}{R}$
x_w	wake station, $\frac{r_w}{R}$
β	blade angle, deg
$\beta_{0.75R}$	blade angle at 0.75R, deg
ρ	air density, slugs/cu ft

Subscripts:

F front propeller

R rear propeller

APPARATUS

Test equipment.- The present tests were conducted in the Langley 8-foot high-speed tunnel with the propeller dynamometer described in references 1 and 2. A sketch of the dynamometer installed in the tunnel is shown in figure 1.

Separate electric motors were used to drive the front and rear propellers but only a single source of variable-frequency power was available for this purpose. The front and rear propeller rotational speeds could not, therefore, be controlled individually. Differences in loading between the front and rear propellers, coupled with differences in the motor characteristics, resulted in unequal rotational speeds of the two propellers. This difference in rotational speed amounted to a maximum of 1.7 percent.

Total pressures in the wake of the propeller were measured by the survey rakes shown in figure 1. The rake struts were sweptback at an angle of 45° and the airfoil section perpendicular to the leading edge had a maximum thickness ratio of 10 percent. The total pressures were measured in a plane approximately 17 inches downstream of the rear propeller center line. The radial locations of the total-pressure tubes were such that the tube locations of one rake were not duplicated by those of the opposite rake. The total-pressure tubes were constructed of stainless-steel tubing with an outside diameter of 0.090 inch. Each tube was reamed with a tapered reamer having an included angle of 20° which produced a nearly sharp leading edge on each total-pressure tube. A slant-type manometer board was used to measure the total pressures and the readings were recorded photographically.

Propeller.- The 3-foot-diameter dual-rotating propeller consisted of eight blades: four in the front propeller and four of opposite hand in the rear propeller. The distance between propeller center lines was 6 inches. The front and rear blades differed slightly in twist, as shown by the blade-form curves of figure 2. In other respects, the design of the front and rear blades was identical. NACA 16-series airfoil sections were used and all sections were cambered for a design lift coefficient of 0.3. The propeller was designed for an unusually high advance ratio of 7.15, which corresponds to a blade angle of about 75° at 0.75R. A photograph of a blade is shown in figure 3.

TESTS AND REDUCTION OF DATA

Each run was made at a fixed value of tunnel Mach number and blade-angle setting, with the rotational speed varied to cover a range of advance ratio. The difference in blade angle between the front and rear propellers was chosen to produce approximately equal power absorption at peak efficiency. Thrust loadings, obtained from the wake surveys, are presented in this report for front propeller blade angles of 65°, 70°, 75°, and 80° measured at 0.75R. The forward Mach number range was varied from 0.35 to 0.925.

The total pressures in the propeller wake were measured by the rakes. With the propeller operating, the radial variation of static pressure at the rake location was found to be small. For simplicity, the static pressure used for determination of the thrust loading was obtained from an orifice on the dynamometer barrel.

The pressure measurements were reduced to section thrust coefficient by means of the equations presented in references 3 and 4. The basic equation for section thrust coefficient for a propeller in free air, obtained from reference 3, is

$$\frac{dC_T}{dx_w} = \frac{\pi J^2 x_w}{2}\left(\frac{\rho_1}{\rho_2}\right)^{1/2}\left(\frac{q_1}{q_0}\right)^{1/2}\left[\left(\frac{q_2}{q_0}\right)^{1/2} - \left(\frac{\rho_2}{\rho_0}\right)^{1/2}\right]$$

where

J advance ratio, $\frac{V_0}{nD}$

q dynamic pressure, $\frac{1}{2}\rho V^2$

ρ air density

V velocity

Subscripts:

0 far ahead of propeller (free stream)

1 at the rake location in the propeller wake

2 far behind propeller (where static pressure has returned to free-stream static pressure)

[redacted]

As pointed out in reference 3, the quantity $\left(\frac{\rho_1}{\rho_2}\right)^{1/2}\left(\frac{q_1}{q_0}\right)^{1/2}$ is a function of M_0, P_1, and $\frac{\Delta H}{q_0}$ where

M_0 free-stream Mach number

P_1 static-pressure coefficient, $\frac{p_1 - p_0}{q_0}$

$\frac{\Delta H}{q_0}$ total-pressure-rise coefficient, $\frac{H_1 - H_0}{q_0}$

p static pressure

H total pressure

Values of $\left(\frac{\rho_1}{\rho_2}\right)^{1/2}\left(\frac{q_1}{q_0}\right)^{1/2}$ were computed for assumed values of M_0, P_1, and $\frac{\Delta H}{q_0}$. These data were then plotted as a family of curves to permit the term $\left(\frac{\rho_1}{\rho_2}\right)^{1/2}\left(\frac{q_1}{q_0}\right)^{1/2}$ to be easily obtained from the measured data.

The quantity $\left(\frac{q_2}{q_0}\right)^{1/2}$ is a function of M_0 and $\frac{\Delta H}{q_0}$. A second set of curves was computed and plotted for this quantity.

The remaining quantity in the basic equation $\left(\frac{\rho_2}{\rho_0}\right)^{1/2}$ is not so tractable. Evaluation of this term by the method suggested in reference 3 requires a knowledge of the stagnation temperature rise through the propeller. Since this information was not obtained in the present tests, the method suggested in reference 4 was used to approximate this density ratio. The expression given in reference 4 is

$$\left(\frac{\rho_2}{\rho_0}\right)^{1/2} = \left(\frac{c_p T_0}{K + c_p T_0}\right)^{1/2}$$

[redacted]

where

$$K \approx \frac{4}{\pi J^3} C_P V_0^2 (1 - \eta)$$

c_p specific heat of air at constant pressure, ft-lb/slug/deg

T_0 absolute temperature (static) of free stream, $^\circ R$

C_P power coefficient, $\frac{P}{\rho n^3 D^5}$

P power, ft-lb/sec

η efficiency

The values of power coefficient and efficiency used in this equation were obtained from the force tests of this propeller (ref. 1). The density ratio obtained from this equation represents an average value along the radius and was felt to be inapplicable at stations where the loading was small. Since the loading is relatively small at the tip station, the density ratio at this station and at all stations beyond the tip was arbitrarily assumed to be unity.

In the present tests, the values substituted in the preceding equations for the free-stream condition were obtained from the wind-tunnel calibration. This calibration was performed with the propeller dynamometer mounted in the tunnel but with the propeller blades removed.

It was not feasible to determine the thrust loading within the boundary layer which existed on the dynamometer barrel. Measurements of section thrust coefficient inboard of $x_w = 0.525$ are, therefore, not presented and no values of the integrated thrust coefficient are presented.

The front and rear propellers generally operated at somewhat different rotational speeds. The values of section thrust coefficient and advance ratio presented herein were based on the rotational speed of the front propeller. The values of advance ratio presented have been corrected for the effect of tunnel-wall constraint as explained in reference 1.

RESULTS AND DISCUSSION

An interesting phenomenon occurred during this dual-rotation test which had not occurred in previous tests of two-blade single-rotating

[redacted]

propellers in the 8-foot high-speed tunnel. This phenomenon took the form of "beats" which were clearly audible in the tunnel test chamber. At a fixed operating condition, the sound level rose and fell at a regular rate with a period ranging from less than a second to several seconds, depending upon the particular operating condition. This fluctuation of the noise level was accompanied by a fluctuation of the wake total pressures as indicated by the manometer-board tubes. The thrust distribution indicated by the total-pressure tubes appeared to be normal when the sound was at a minimum but was considerably distorted when the "beat" noise was at a maximum. The two conditions are illustrated by figure 4 for a front propeller blade angle of 70° at a forward Mach number of 0.35.

The "beat" noise and the distortion of the wake pattern have not been explained but it seems likely that they are connected with the difference in rotational speeds of the two propellers. The "beat" effect occurred over the complete Mach number range but was apparent only at operating conditions near peak efficiency. The frequency of the beat varied with rotational speed at a given blade angle and Mach number and appeared to be a function of the difference in rotational speed of the front and rear components, becoming smaller as the difference in speed became smaller.

This "beat" effect would probably not occur in a normal dual-propeller installation where the two propellers are geared to turn at the same rotational speed. An attempt has, therefore, been made to eliminate the distorted thrust distributions from the following data.

Figures 5 to 8 present the measured section-thrust-coefficient curves for the NACA 3-(3)(05)-05 eight-blade dual propeller at blade-angle settings for the front propeller of 65°, 70°, 75°, and 80°. The test points shown were obtained from both rakes. In most cases, good agreement was obtained between the two rakes.

The thrust loading curves resemble those for single-rotating propellers, although the thrust on the inboard stations is presumably higher than would be attained by a single-rotating propeller of optimum loading, for the dual propeller was designed to produce such a higher loading. In many cases, the influence of the propeller extends well beyond the station that equals the propeller-tip radius ($x_w = 1.0$).

The effects of compressibility on the thrust loading of the dual propeller will be illustrated primarily by the data at a front-propeller blade-angle setting of 75° since this is very near the design angle. Figure 9 shows the effect of forward Mach number on the section-thrust-coefficient loading at an advance ratio J_F of 7.3, which is the advance ratio for peak efficiency at the lower test forward speeds. As the forward Mach number is increased from 0.35 to 0.80, there is a progressive

increase in the value of $\frac{dC_T}{dx_w}$ over the entire blade. At Mach numbers above 0.80, the section thrust coefficient drops rapidly, but the decrease is less pronounced at the outboard stations. The result is that at the highest Mach number tested, the sections near the propeller tip produce a relatively large part of the total thrust.

The loss in thrust coefficient at Mach numbers above 0.80 may be explained as caused by a combination of changes in airfoil section characteristics which take place at Mach numbers beyond the critical speed. These changes may include an increase in drag coefficient, a loss in lift-curve slope, and a shift in the angle of zero lift. A clearer picture of the effects of changes in airfoil characteristics on the thrust can be obtained from figure 10 which shows the variation of section thrust coefficient with advance ratio for several forward Mach numbers. Data are shown for the three radial stations $x_w = 0.525$, 0.70, and 0.90. In general, the curves indicate that increasing the Mach number from 0.35 to 0.80 produces a progressive increase in slope of the curves with little change in the value of the advance ratio for which the thrust is zero. At a Mach number of 0.85, the thrust curves suffer some loss in slope, particularly at the $x_w = 0.70$ station, but this is largely recovered at the highest test Mach numbers of 0.90 and 0.925. The thrust curves at these latter Mach numbers are characterized by a shift in the value of J_F for which the thrust is zero. This shift appears related to the change that takes place in the angle for zero lift of cambered airfoils at Mach numbers beyond the force break. However, at high blade angles, the value of section thrust is greatly affected by a change in the value of section drag coefficient. Much of the shift in the thrust curves to smaller values of advance ratio may therefore be the result of the section drag rise which occurs at high section Mach numbers.

The data indicate, then, that changes in the lift-curve slopes of the airfoil sections have a secondary influence in producing the large decreases in thrust loading which occur at high Mach numbers. These losses in thrust at a constant advance ratio are primarily the result of changes in the angles of zero lift and increases in the drag coefficients of the airfoil sections.

Inspection of figure 10 shows that the changes in thrust loading are less pronounced for the $x_w = 0.90$ station than for the inboard stations. This suggests that a tip-relief effect exists which reduces the shock strength and flow separation near the tip at supercritical speeds and results in lower drag coefficients at the tip sections than at the inboard sections. However, the smaller changes in load near the tip cannot be attributed to tip relief alone, for the smaller aerodynamic helix angles near the propeller tip will tend to decrease the changes in

thrust loading resulting from changes in the aerodynamic characteristics of the airfoil sections.

The effect of compressibility on the thrust loading for operation at maximum efficiency is shown in figure 11 for the four front-propeller blade angles of 65°, 70°, 75°, and 80°. The changes which take place in the loading are similar to those which have been found in tests of single-rotating propellers (ref. 5). As the forward Mach number is increased, the section thrust coefficient increases along the entire blade until a maximum is reached. As the Mach number is increased further, a loss in section thrust coefficient is evident, beginning near the tip and progressing inboard. The Mach number at which this first loss in thrust loading occurs tends to coincide with the beginning of the efficiency loss at high speeds as determined by the force tests of this propeller (ref. 1). At the highest test Mach numbers of 0.90 and 0.925, the advance ratio at which maximum efficiency occurs shifts to smaller values and the outboard sections regain the initial thrust-coefficient loss. At these highest speeds, the thrust is then concentrated farther outboard than at lower speeds. This greater effectiveness of the outboard sections is attributed in part to tip relief which alleviates compression shock and flow separation.

CONCLUSIONS

Wake-survey measurements of the thrust loading of the NACA 3-(3)(05)-05 eight-blade dual-rotating propeller at forward Mach numbers from 0.35 to 0.925 indicate the following:

1. Changes in the lift-curve slopes of the airfoil sections have a secondary influence in producing the large decreases in thrust loading which occur at high Mach numbers for a given advance ratio.

2. The decreases in thrust at high Mach numbers are primarily the result of changes in the angles of zero lift and increases in the drag coefficients of the airfoil sections.

3. The changes in thrust loading with Mach number are less pronounced at the tip sections than at the inboard sections.

Langley Aeronautical Laboratory,
National Advisory Committee for Aeronautics,
Langley Field, Va.

[redacted]

REFERENCES

1. Platt, Robert J., Jr., and Shumaker, Robert A.: Investigation of the NACA 3-(3)(05)-05 Eight-Blade Dual Rotating Propeller at Forward Mach Numbers to 0.925. NACA RM L50D21, 1950.

2. Delano, James B., and Carmel, Melvin M.: Investigation of the NACA 4-(5)(08)-03 Two-Blade Propeller at Forward Mach Numbers to 0.925. NACA RM L9G06a, 1949.

3. Baals, Donald D., and Mourhess, Mary J.: Numerical Evaluation of the Wake-Survey Equations for Subsonic Flow Including the Effect of Energy Addition. NACA ARR L5H27, 1945.

4. Vogeley, A. W.: Flight Measurements of Compressibility Effects on a Three-Blade Thin Clark Y Propeller Operating at Constant Advance-Diameter Ratio and Blade Angle. NACA ACR 3G12, 1943.

5. Harrison, Daniel E. and Mililllo, Joseph R.: The Effect of Thickness Ratio on Section Thrust Distribution as Determined From a Study of Wake Surveys of the NACA 4-(0)(03)-045 and 4-(0)(08)-045 Two-Blade Propellers up to Forward Mach Numbers of 0.925. NACA RM L51B05, 1951.

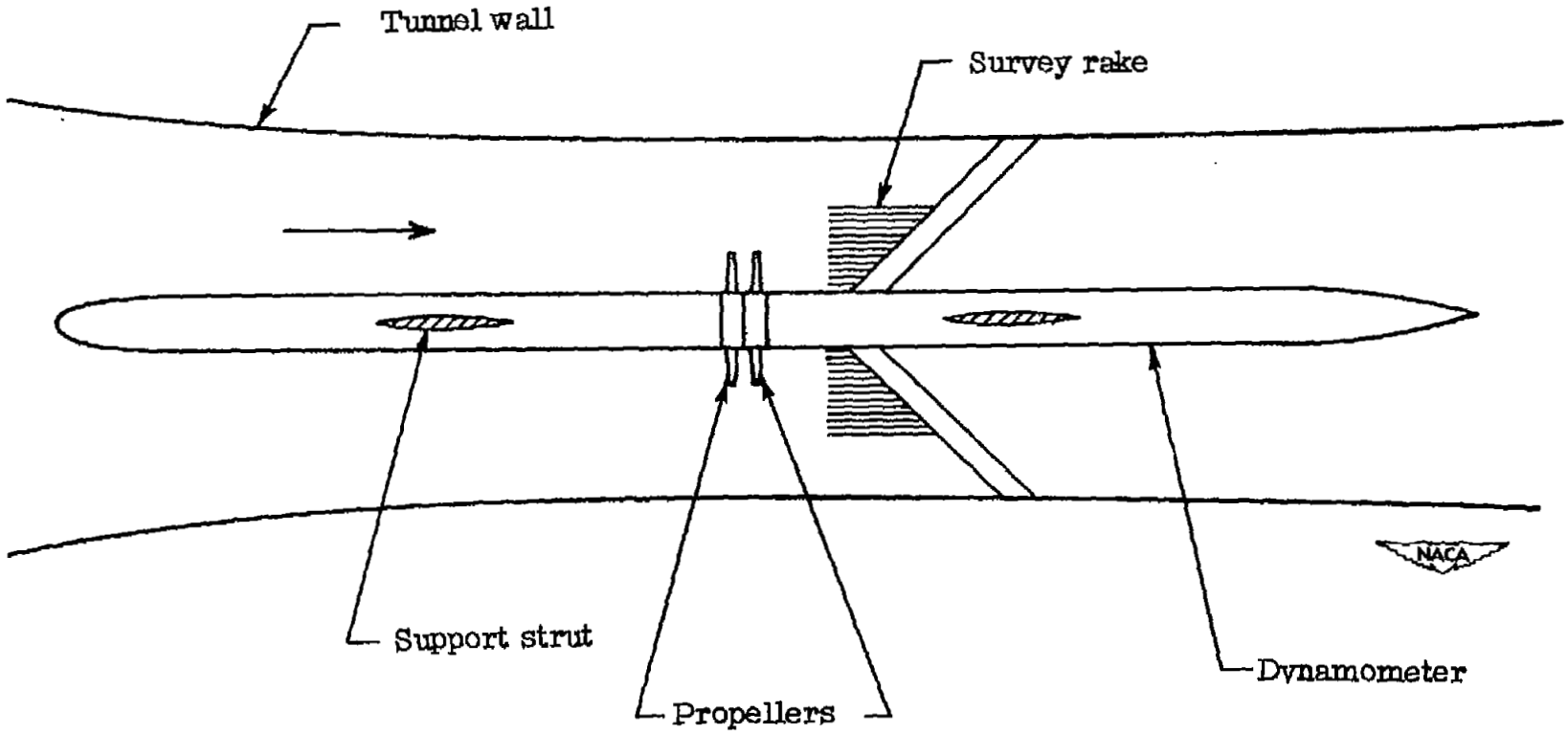

Figure 1.- Top view of test apparatus.

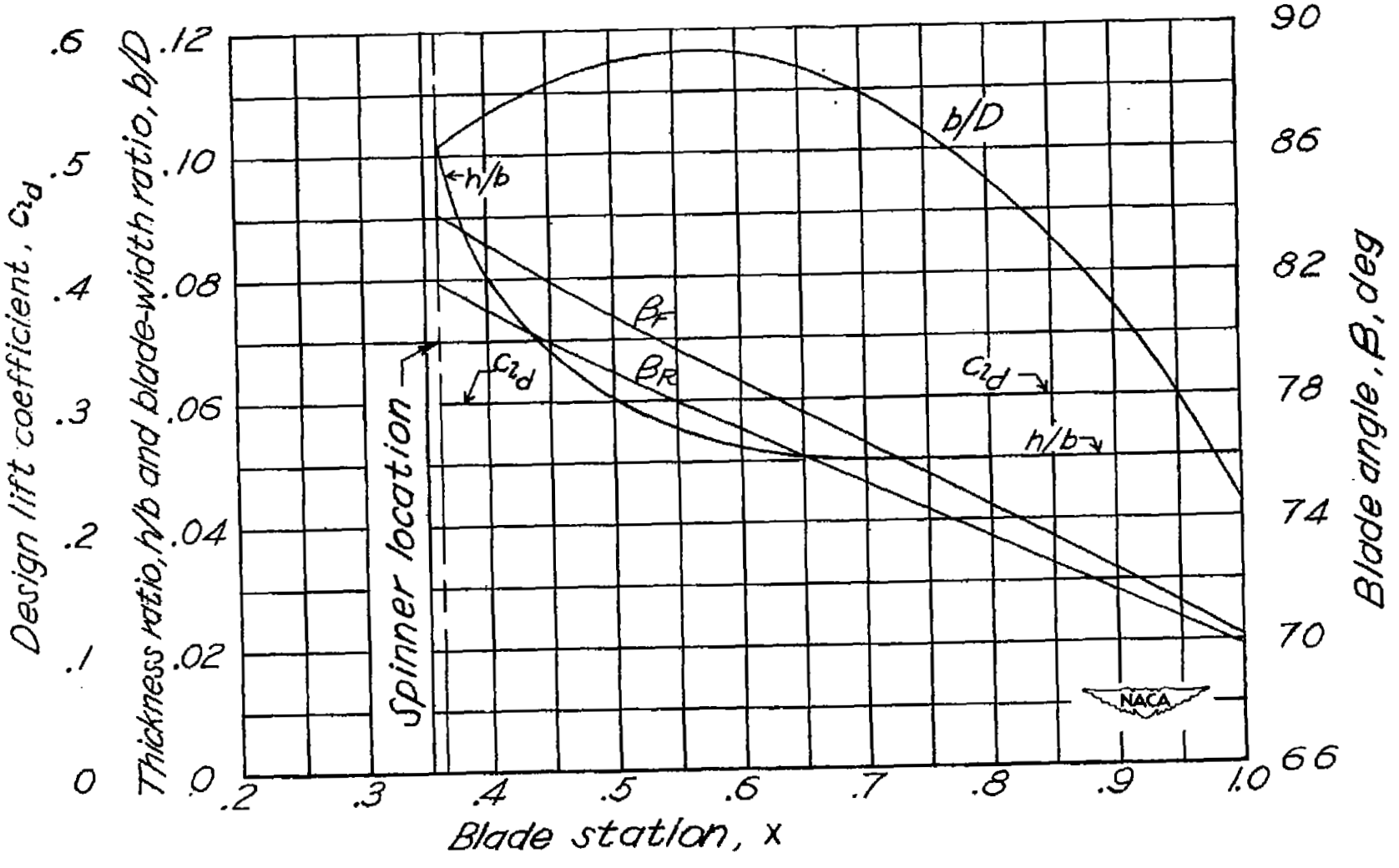

Figure 2.- Blade-form curves for NACA 3-(3)(05)-05 dual propeller.

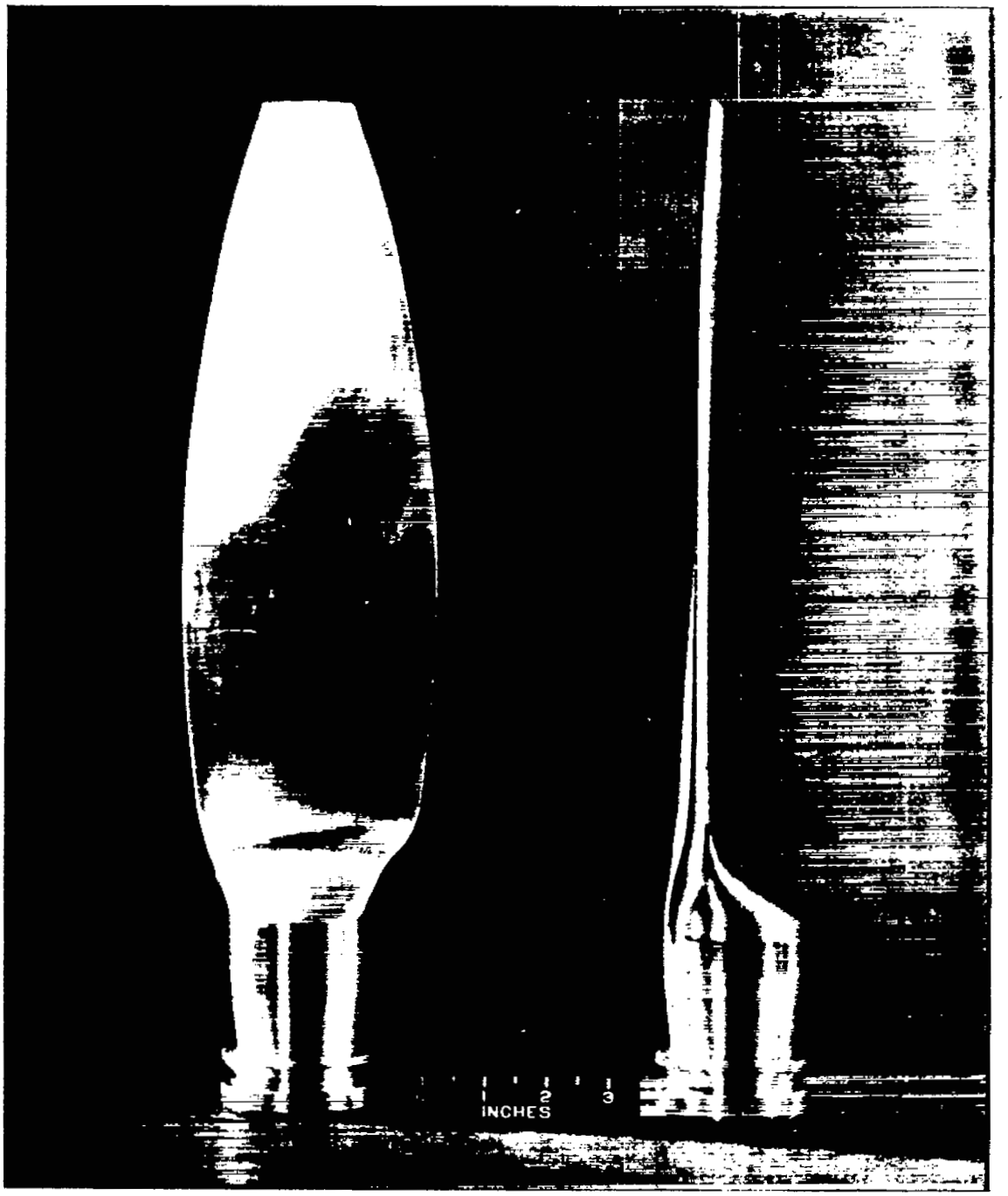

Figure 3.- NACA 3-(3)(05)-05 propeller blade.

NACA
L-64668

[redacted]

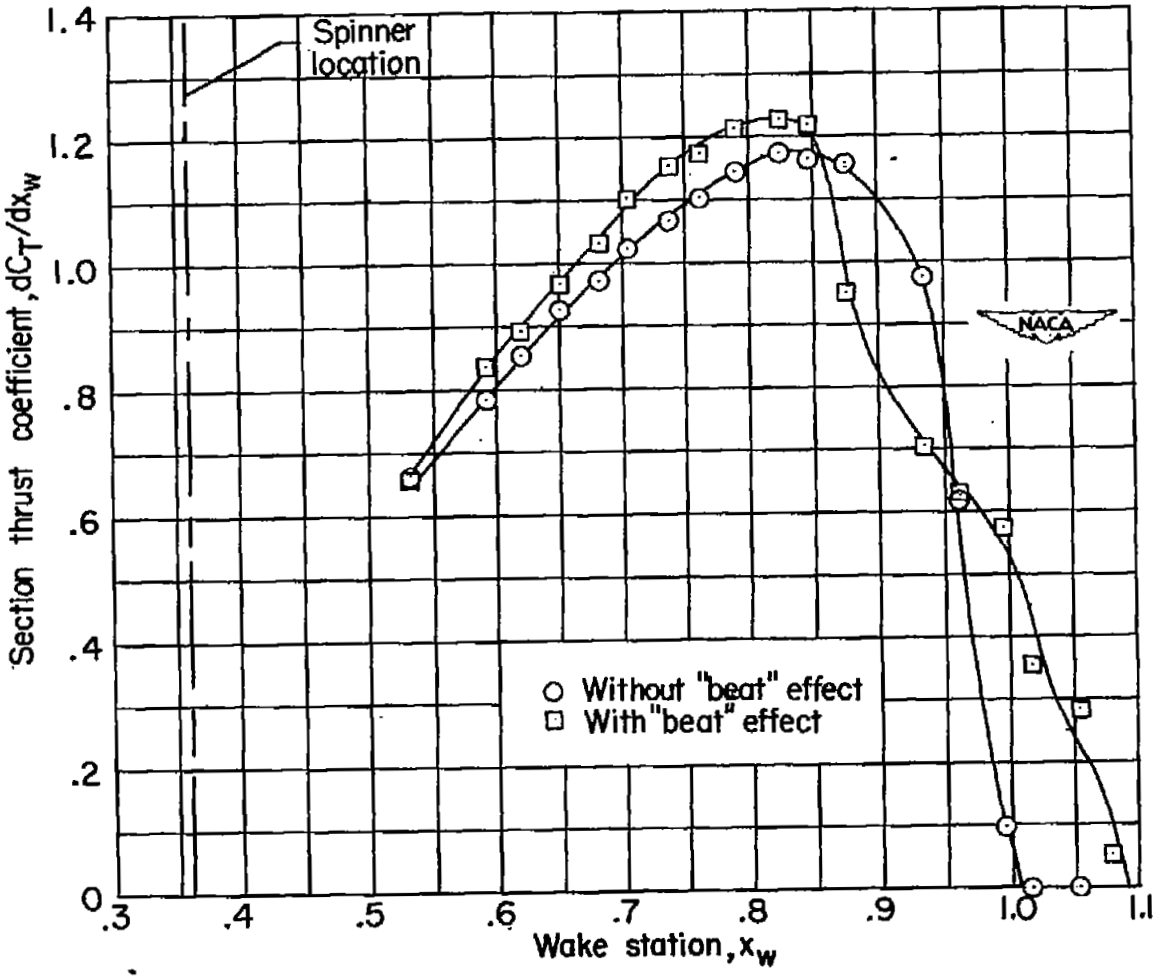

Figure 4.- Comparison of section-thrust-coefficient curves with and without "beat" effect. $\beta_{F_{0.75R}} = 70°$; $\beta_{R_{0.75R}} = 68.2°$; M = 0.35; $J_F = 5.18$.

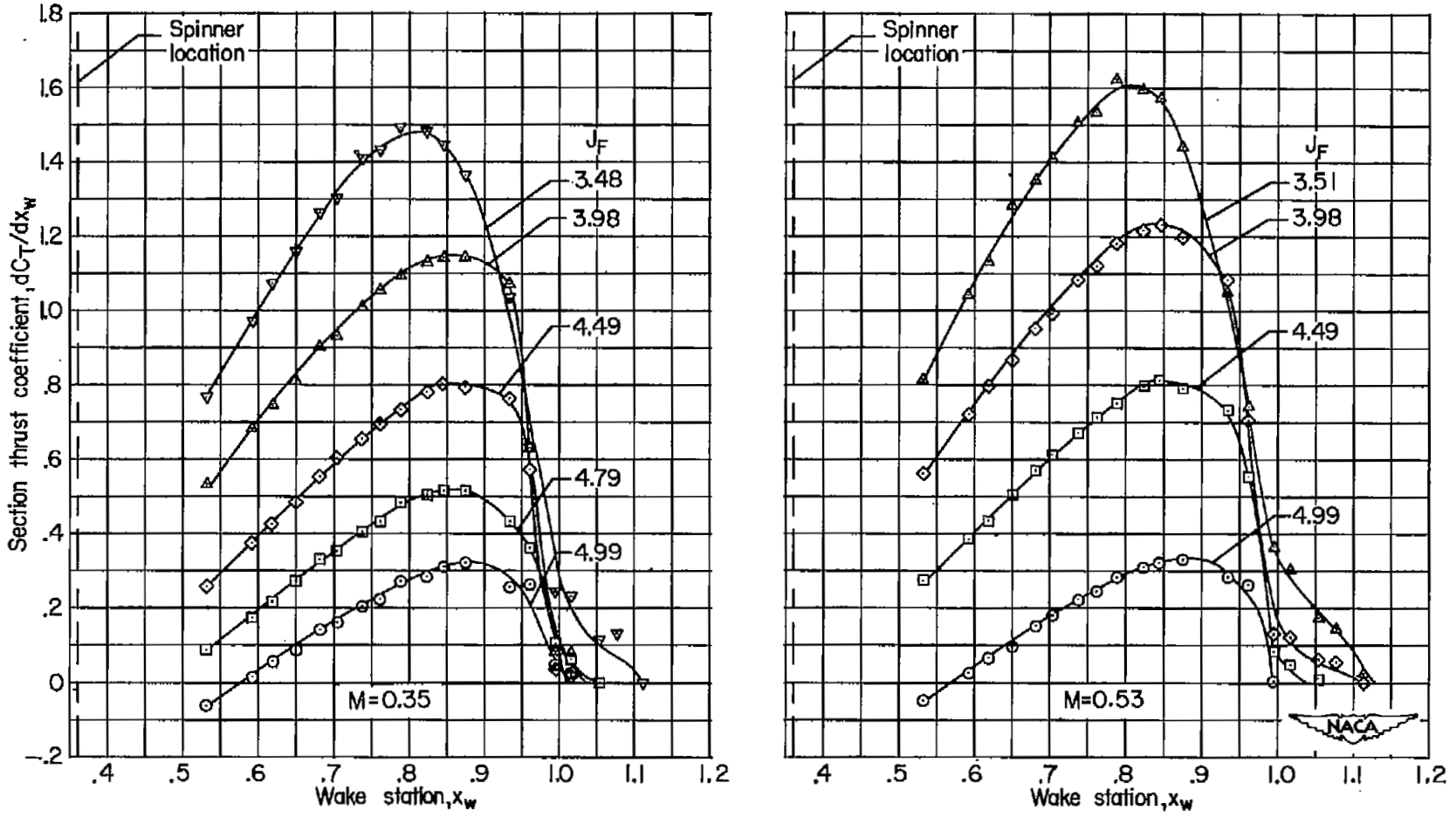

(a) M = 0.35 and 0.53.

Figure 5.- Section-thrust-coefficient curves for NACA 3-(3)(05)-05 eight-blade dual-rotating propeller. $\beta_{F_{0.75R}} = 65°$; $\beta_{R_{0.75R}} = 63.3°$.

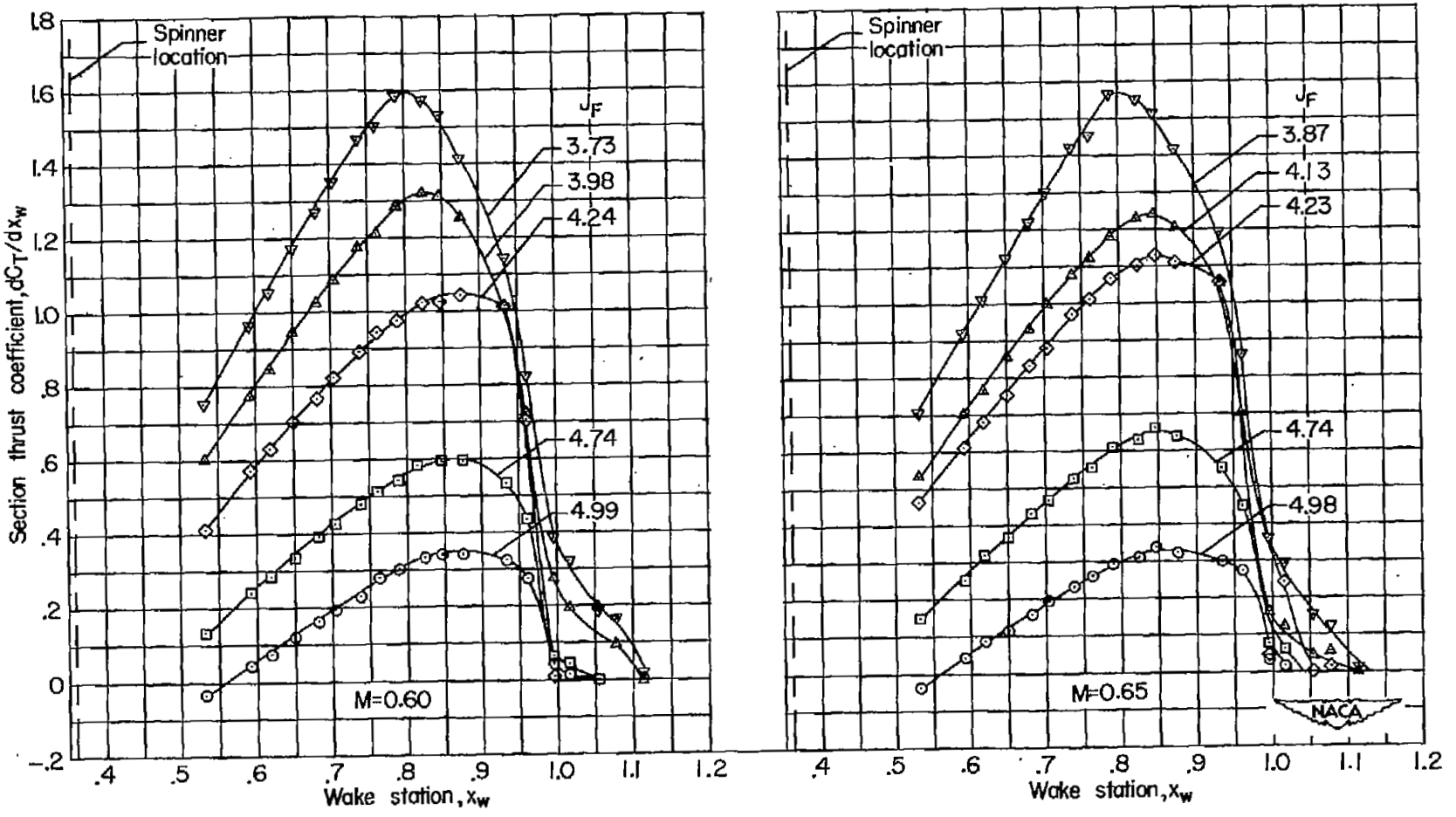

(b) M = 0.60 and 0.65.

Figure 5.- Continued.

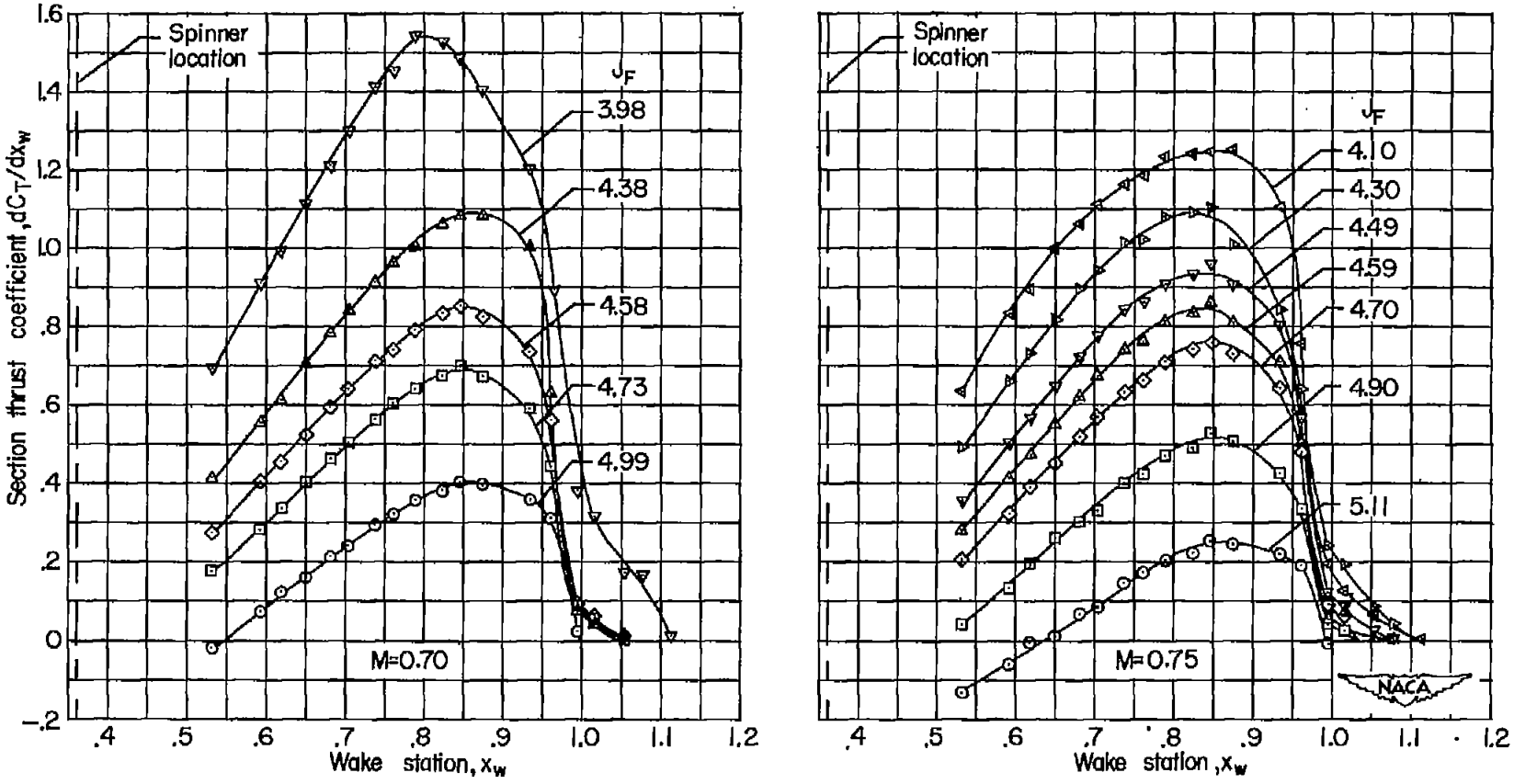

(c) M = 0.70 and 0.75.

Figure 5.- Continued.

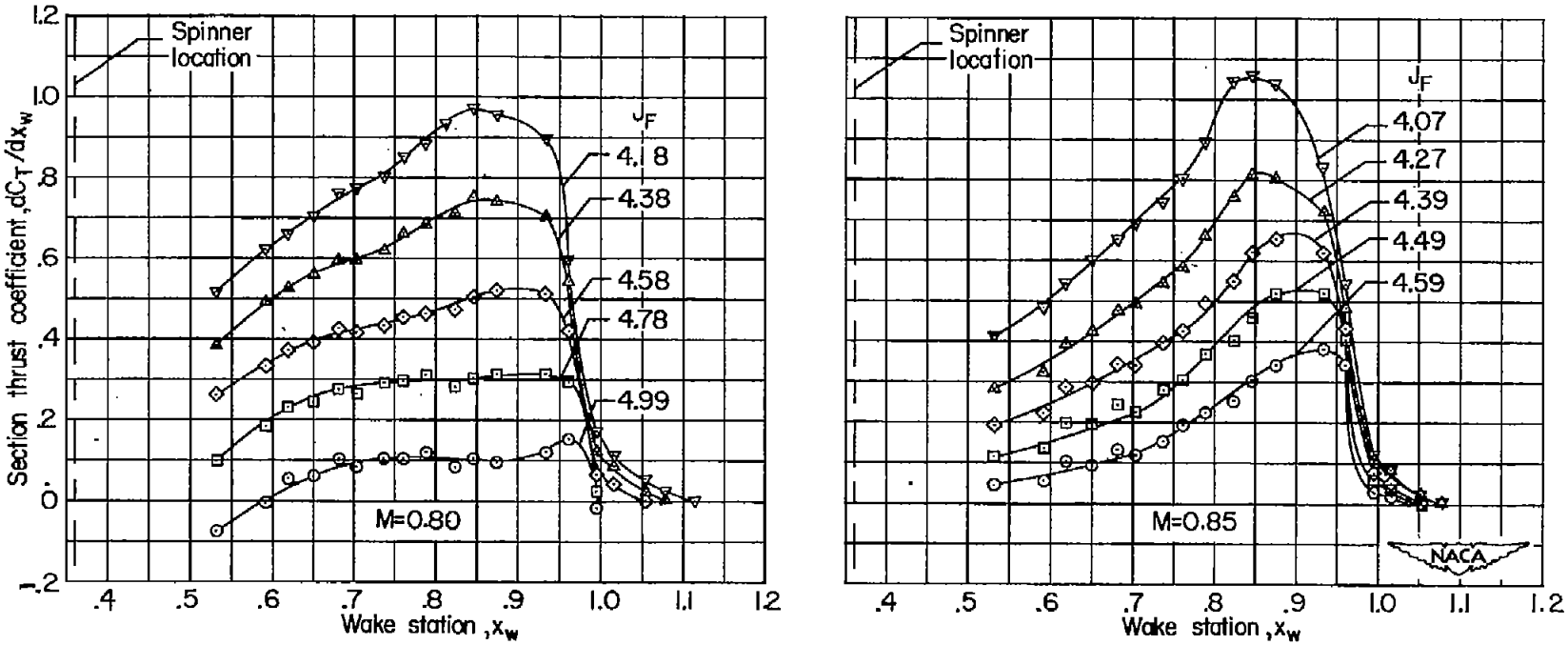

(d) M = 0.80 and 0.85.

Figure 5.- Continued.

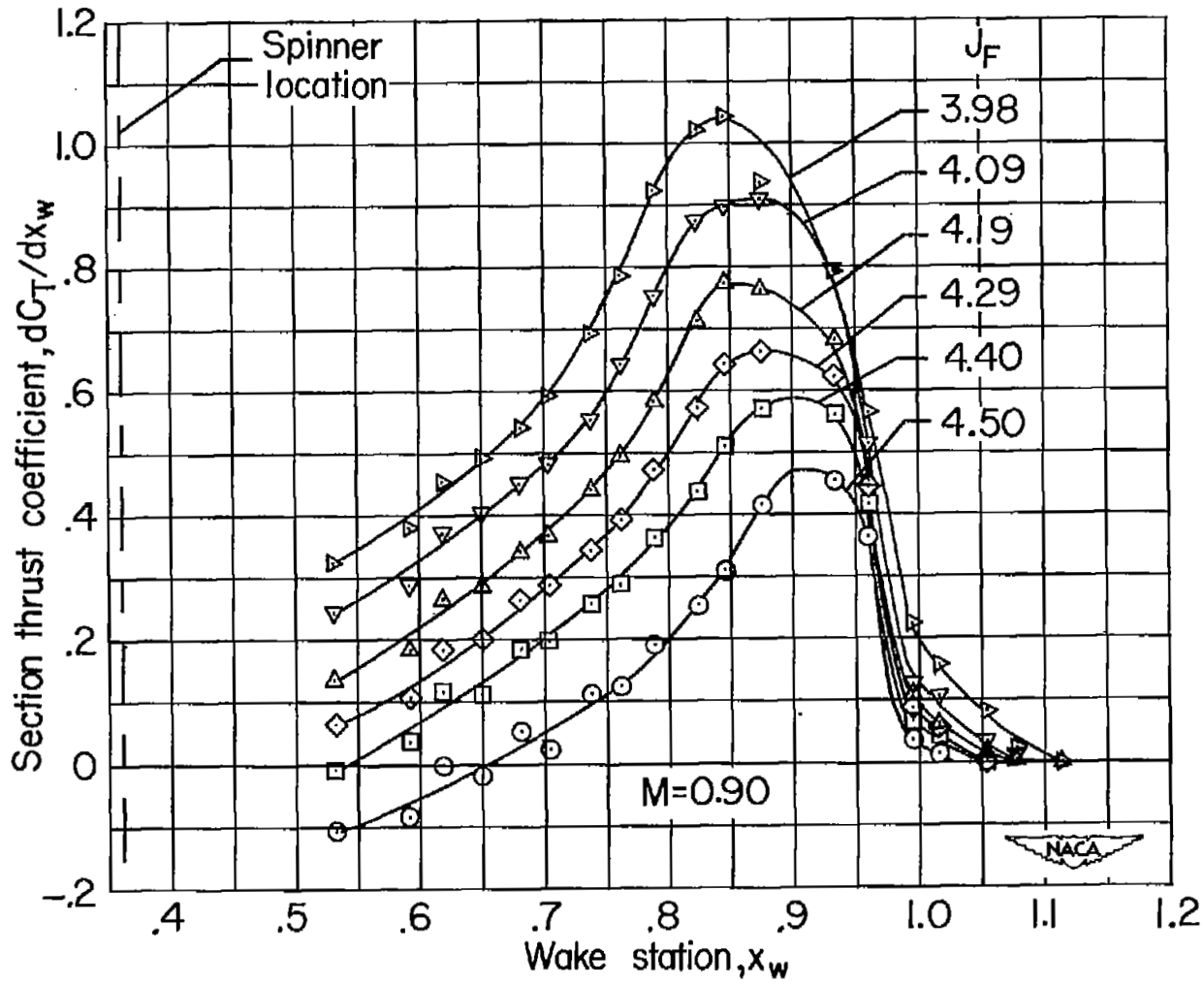

(e) M = 0.90.

Figure 5.- Concluded.

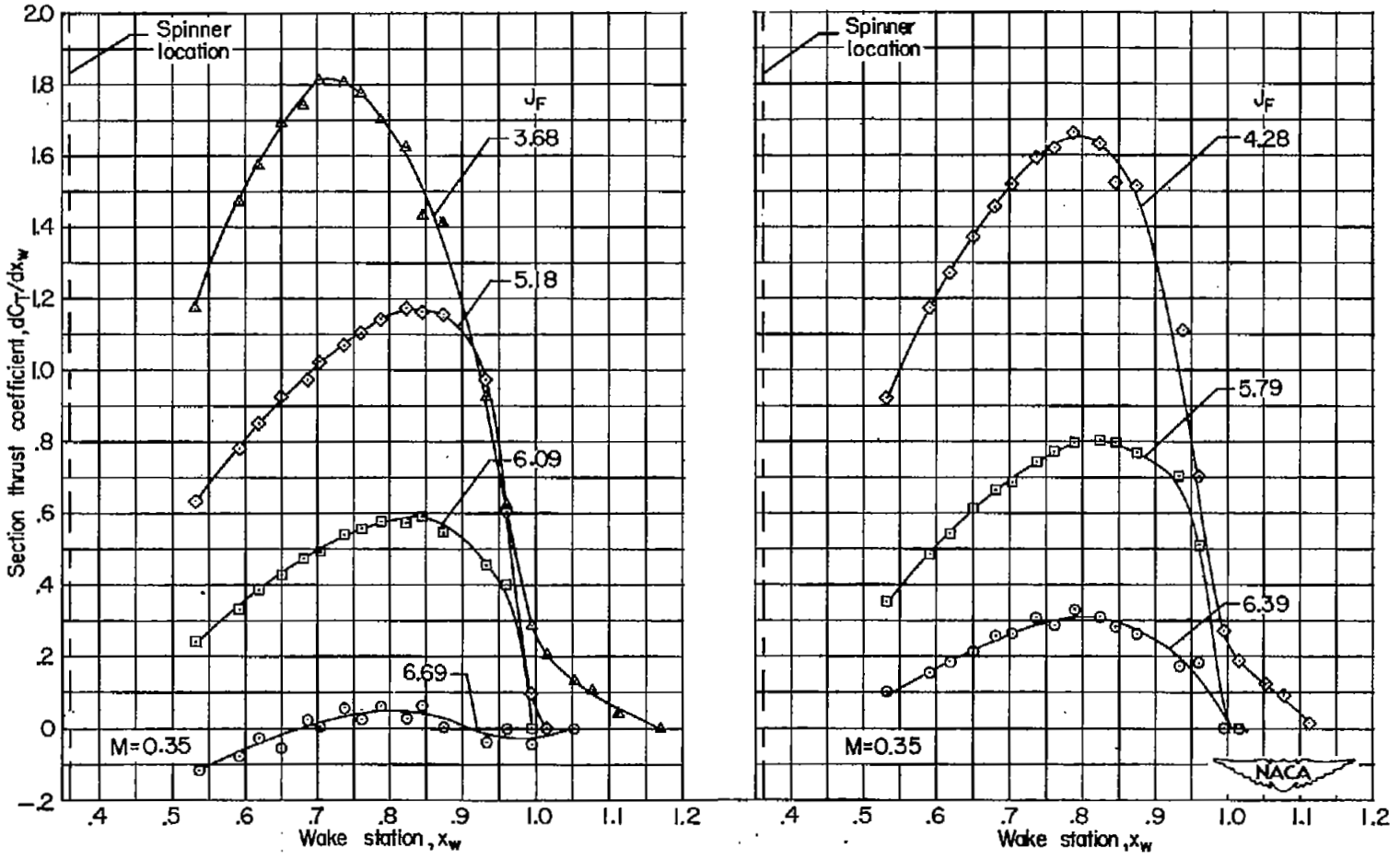

(a) M = 0.35.

Figure 6.- Section-thrust-coefficient curves for NACA 3-(3)(05)-05 eight-blade dual-rotating propeller. $\beta_{F_{0.75R}} = 70^\circ$; $\beta_{R_{0.75R}} = 68.2^\circ$.

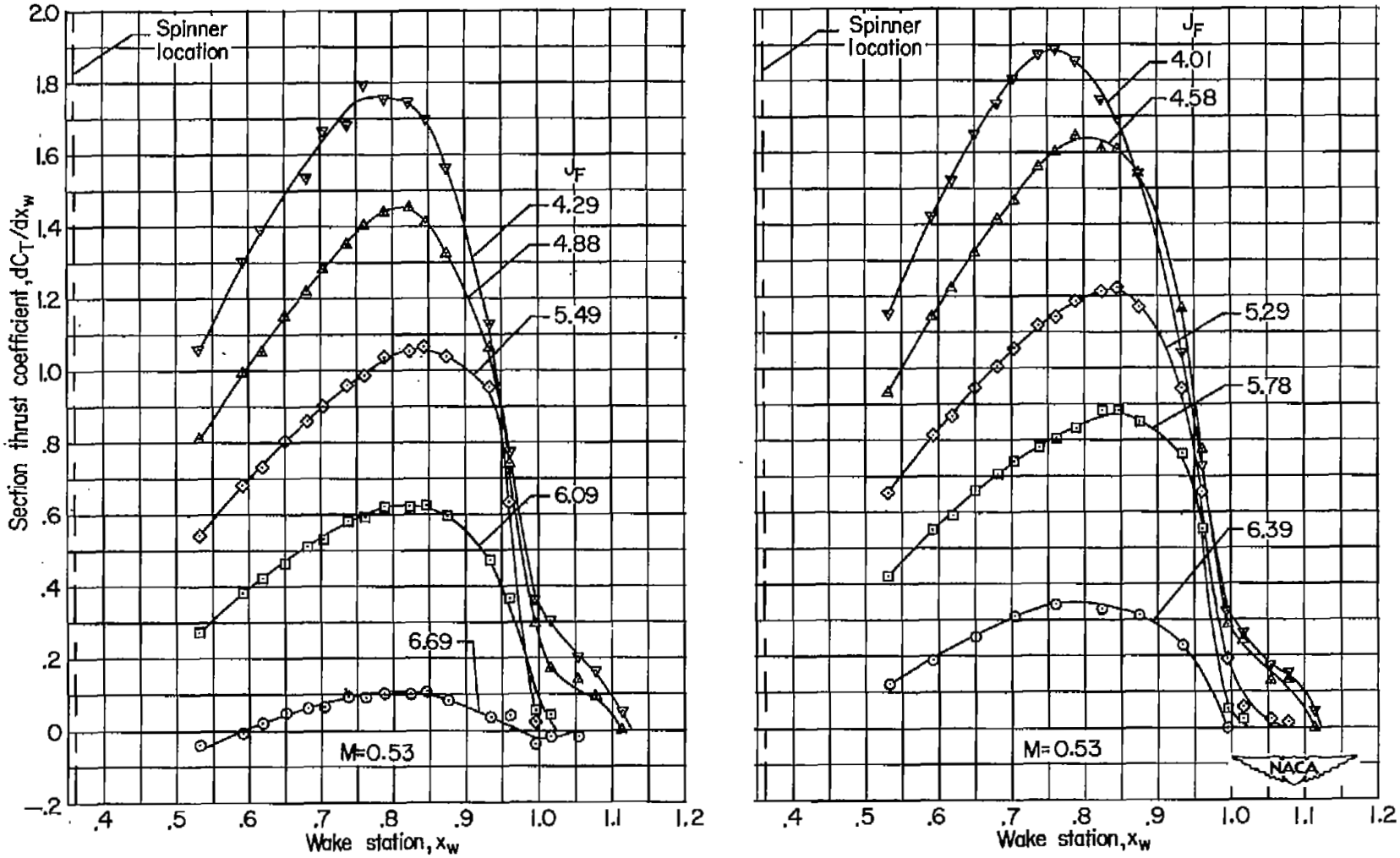

(b) M = 0.53.

Figure 6.- Continued.

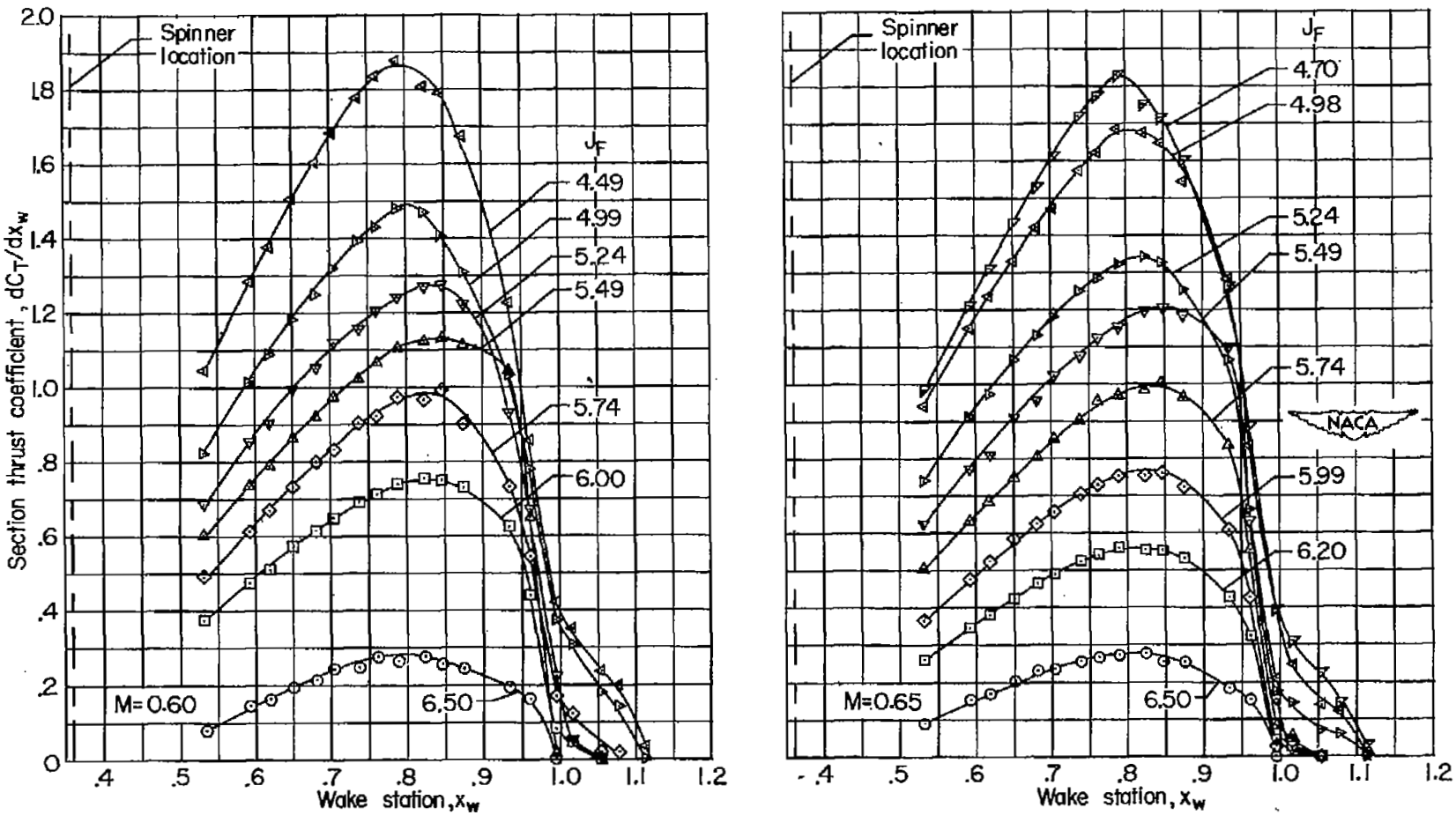

(c) M = 0.60 and 0.65.

Figure 6.- Continued.

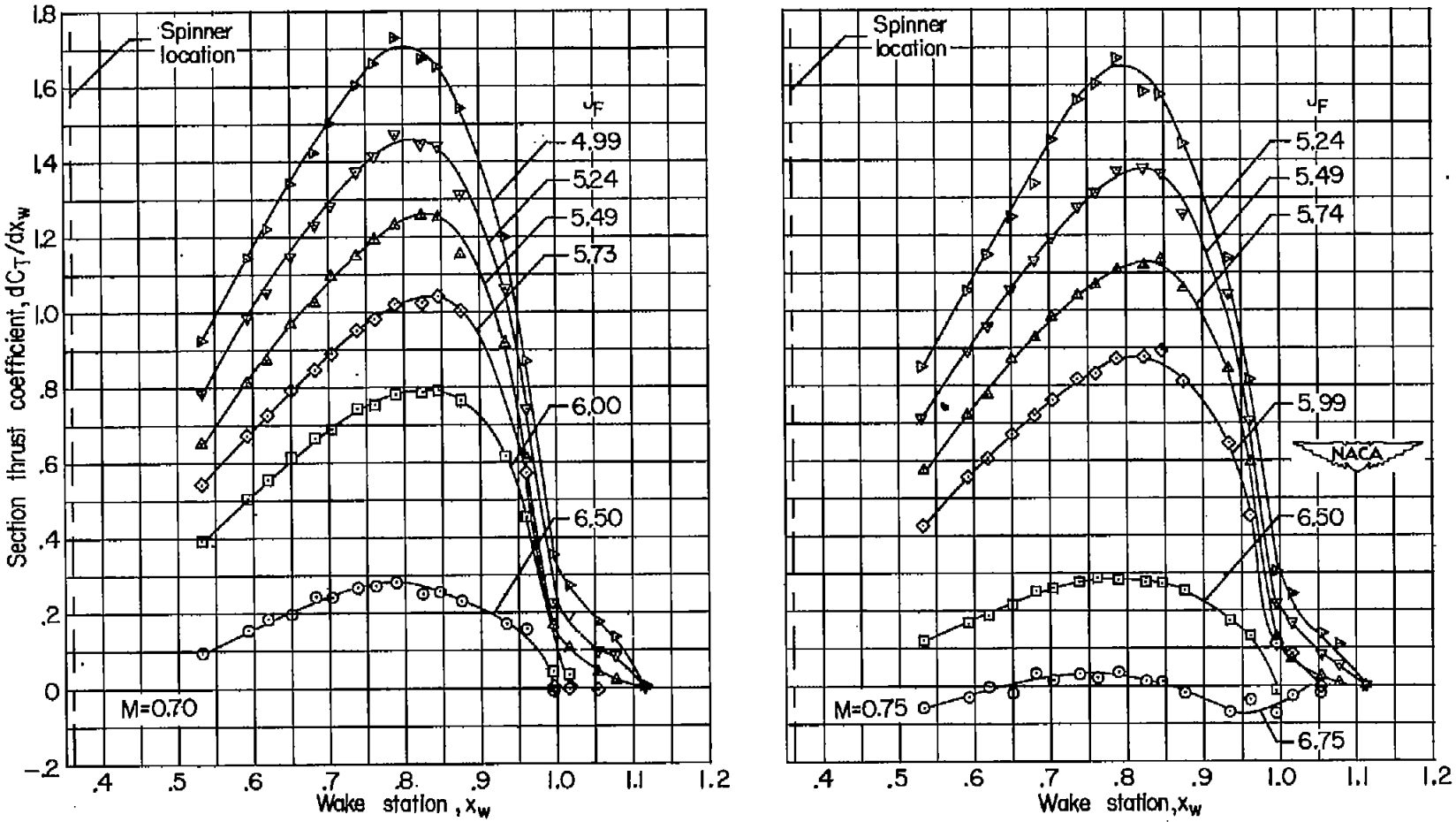

(d) M = 0.70 and 0.75.

Figure 6.- Continued.

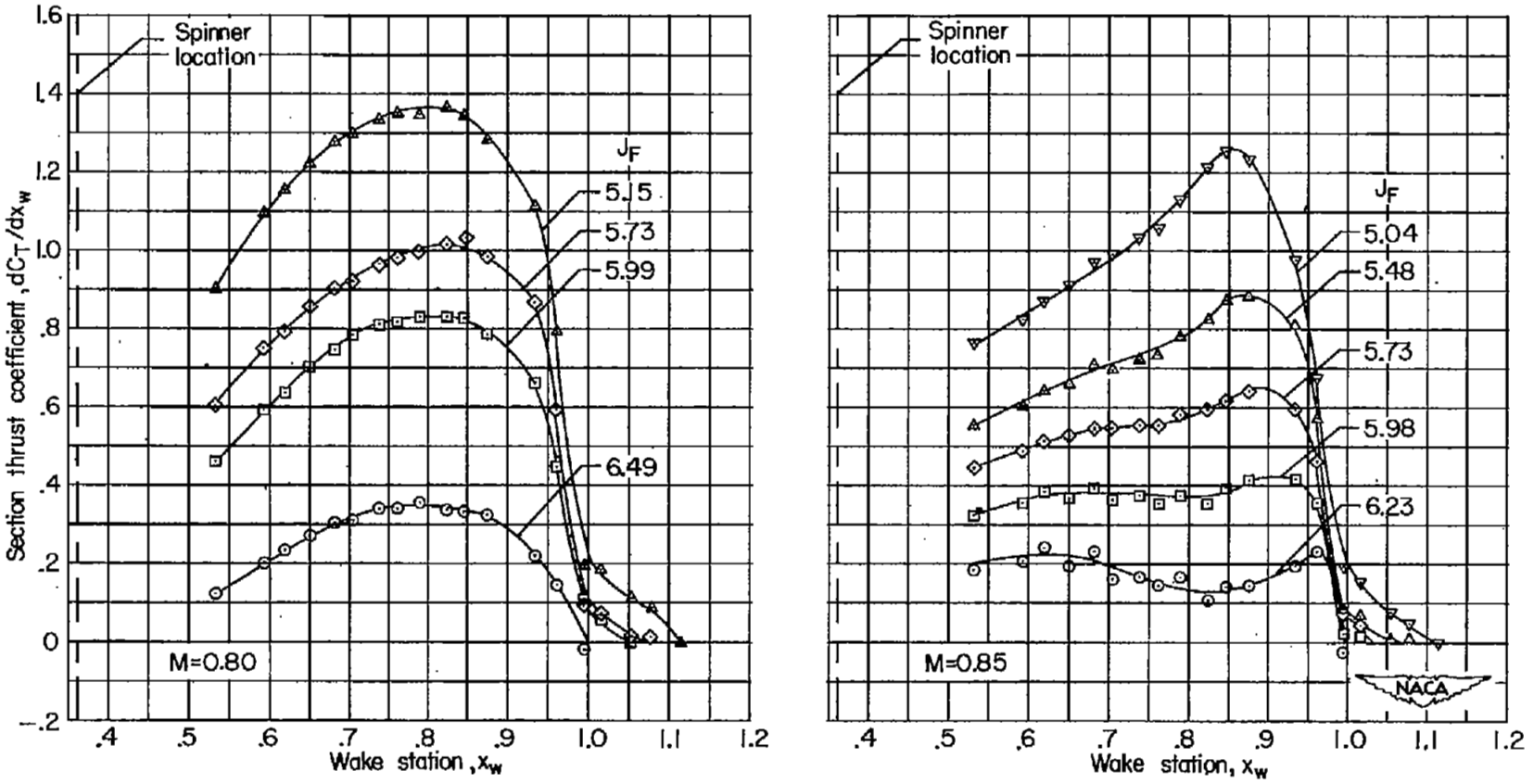

(e) M = 0.80 and 0.85.

Figure 6.- Continued.

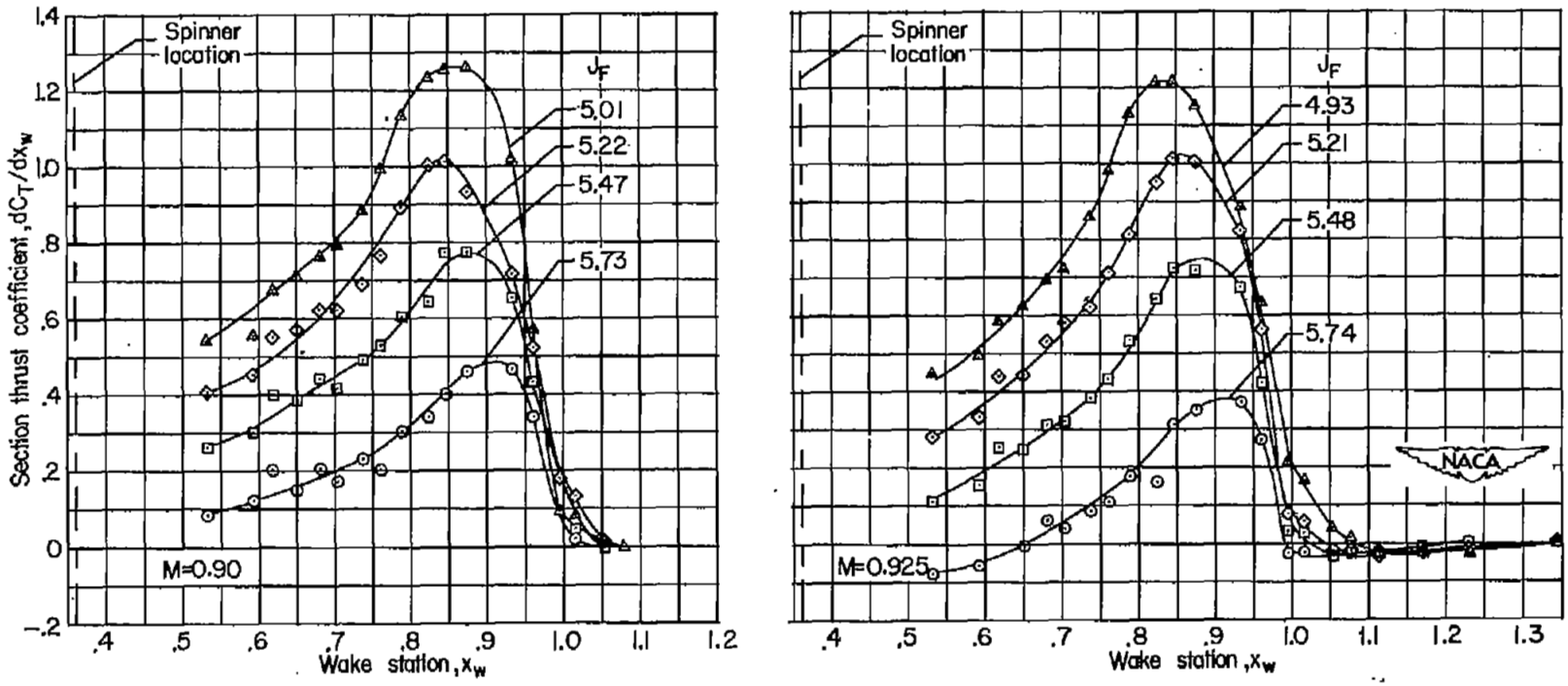

(f) M = 0.90 and 0.925.

Figure 6.- Concluded.

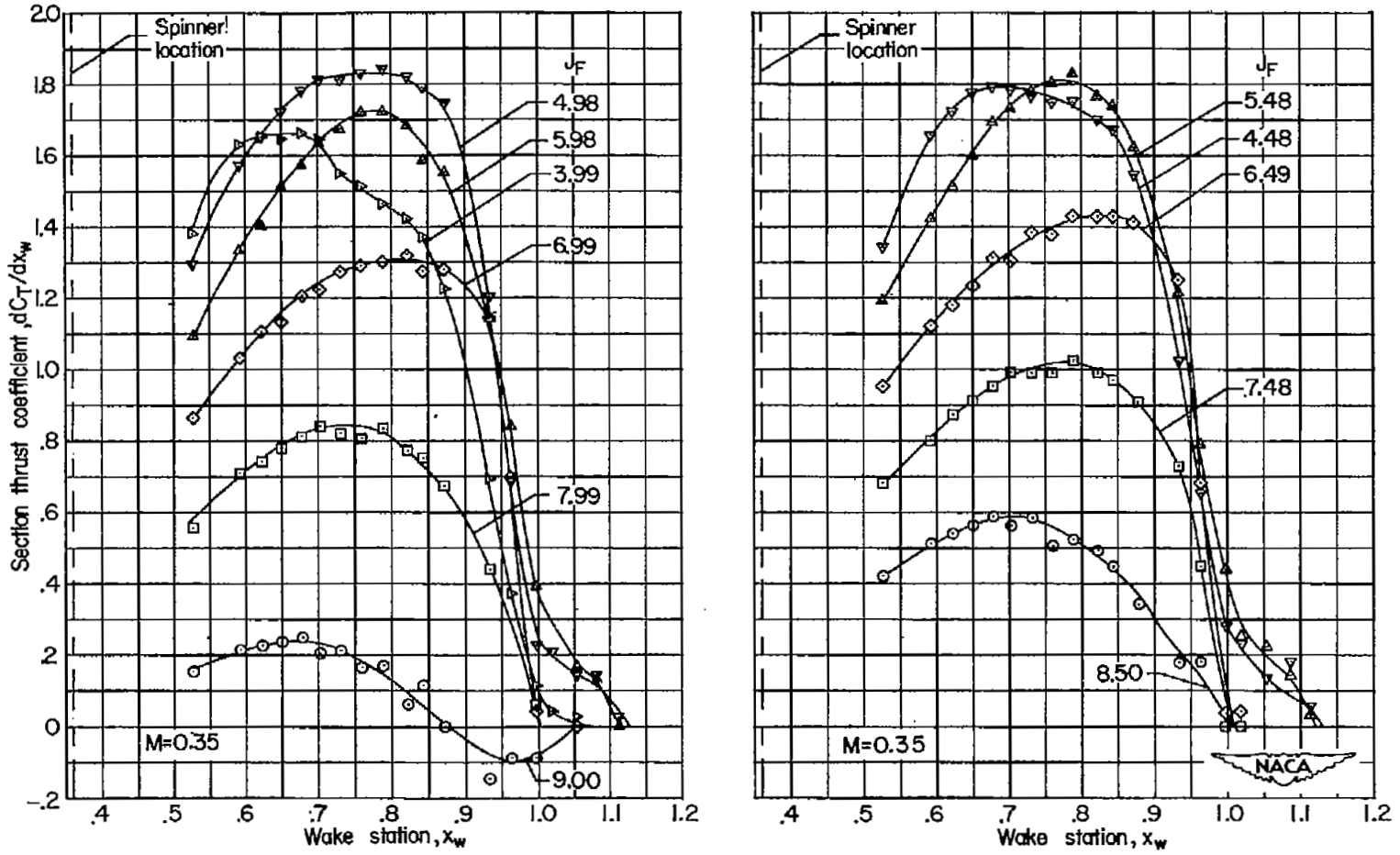

(a) M = 0.35.

Figure 7.- Section-thrust-coefficient curves for NACA 3-(3)(05)-05 eight-blade dual-rotating propeller. $\beta_{F_{0.75R}} = 75^\circ$; $\beta_{R_{0.75R}} = 73^\circ$.

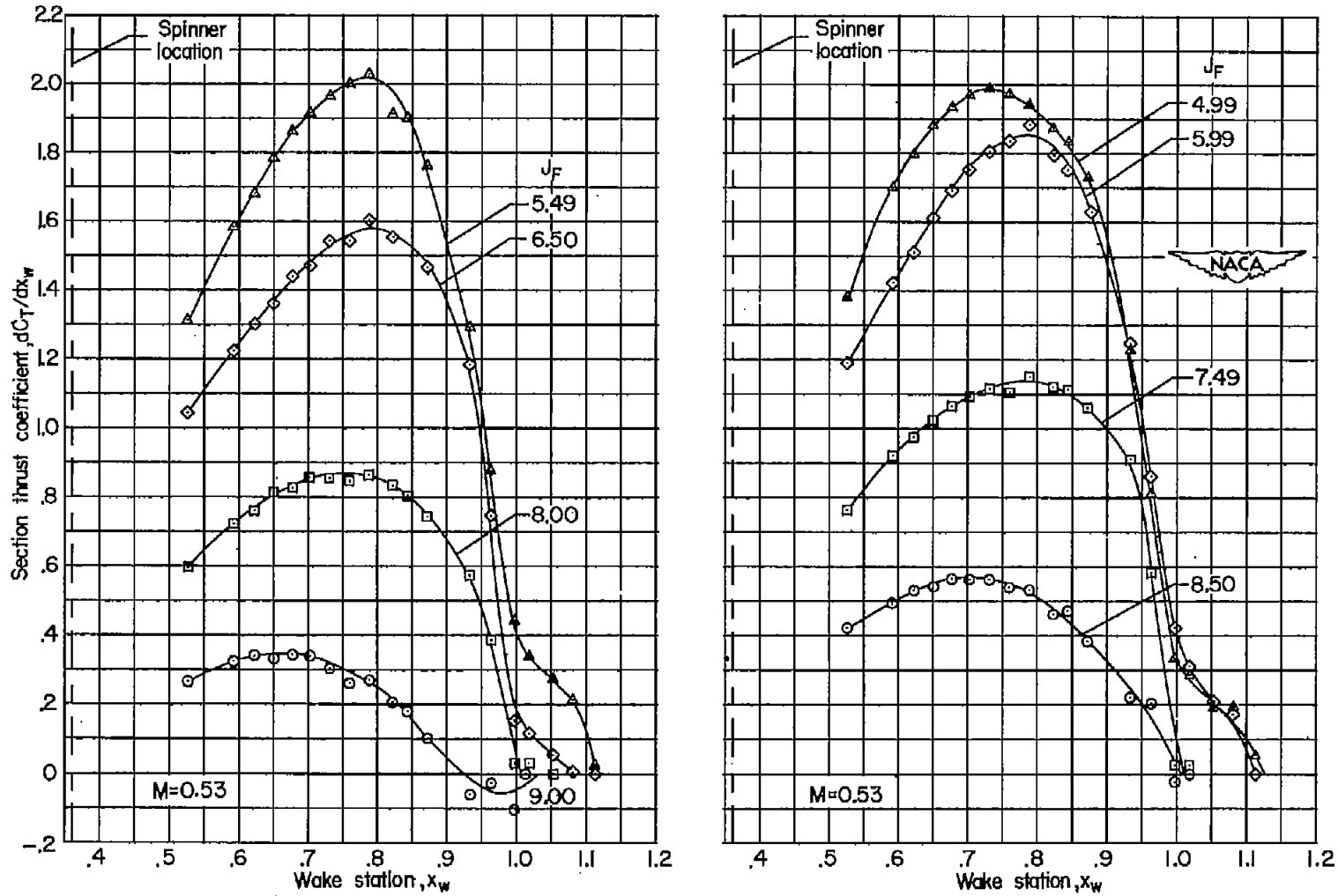

(b) M = 0.53.

Figure 7.- Continued.

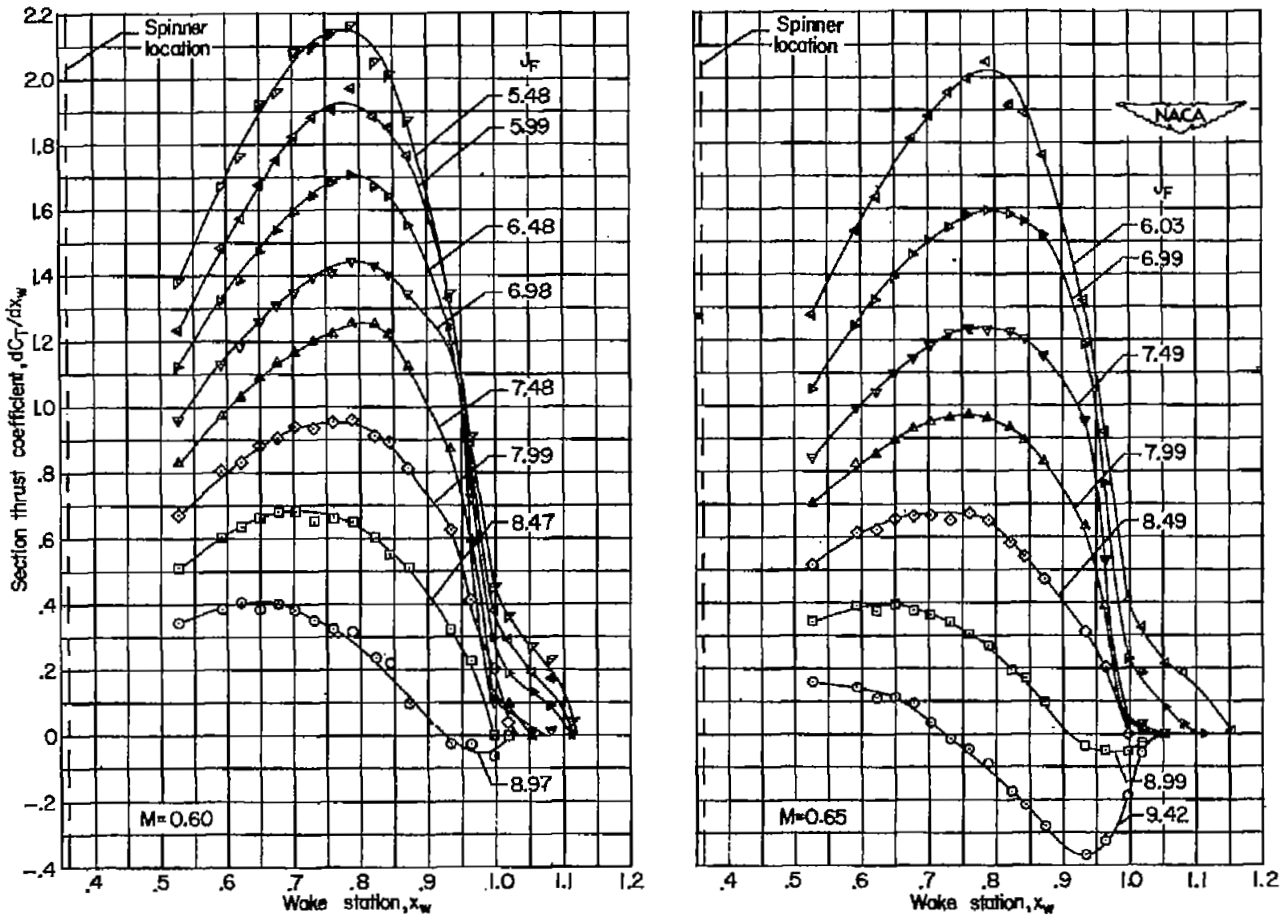

(c) M = 0.60 and 0.65.

Figure 7.- Continued.

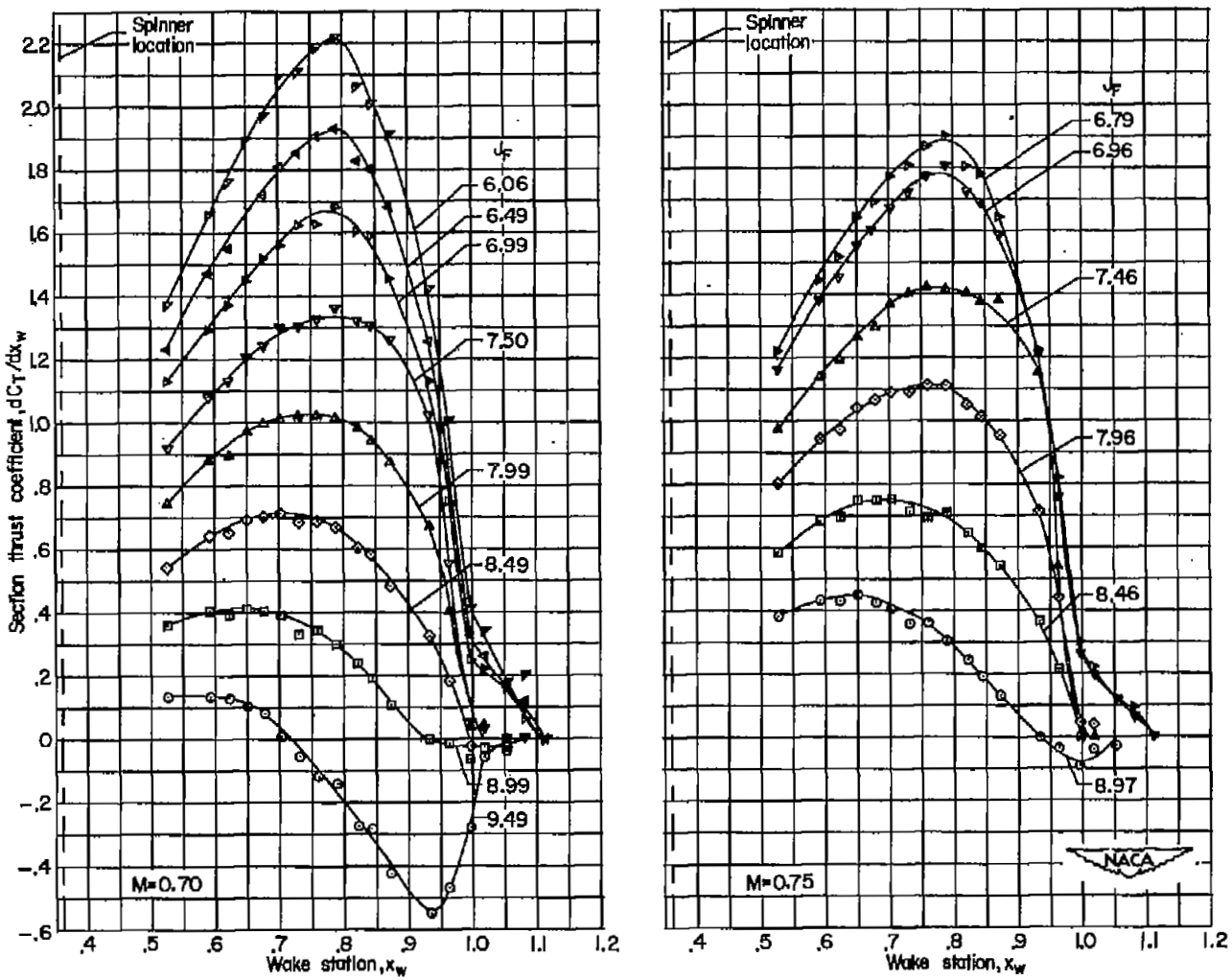

(d) M = 0.70 and 0.75.

Figure 7.- Continued.

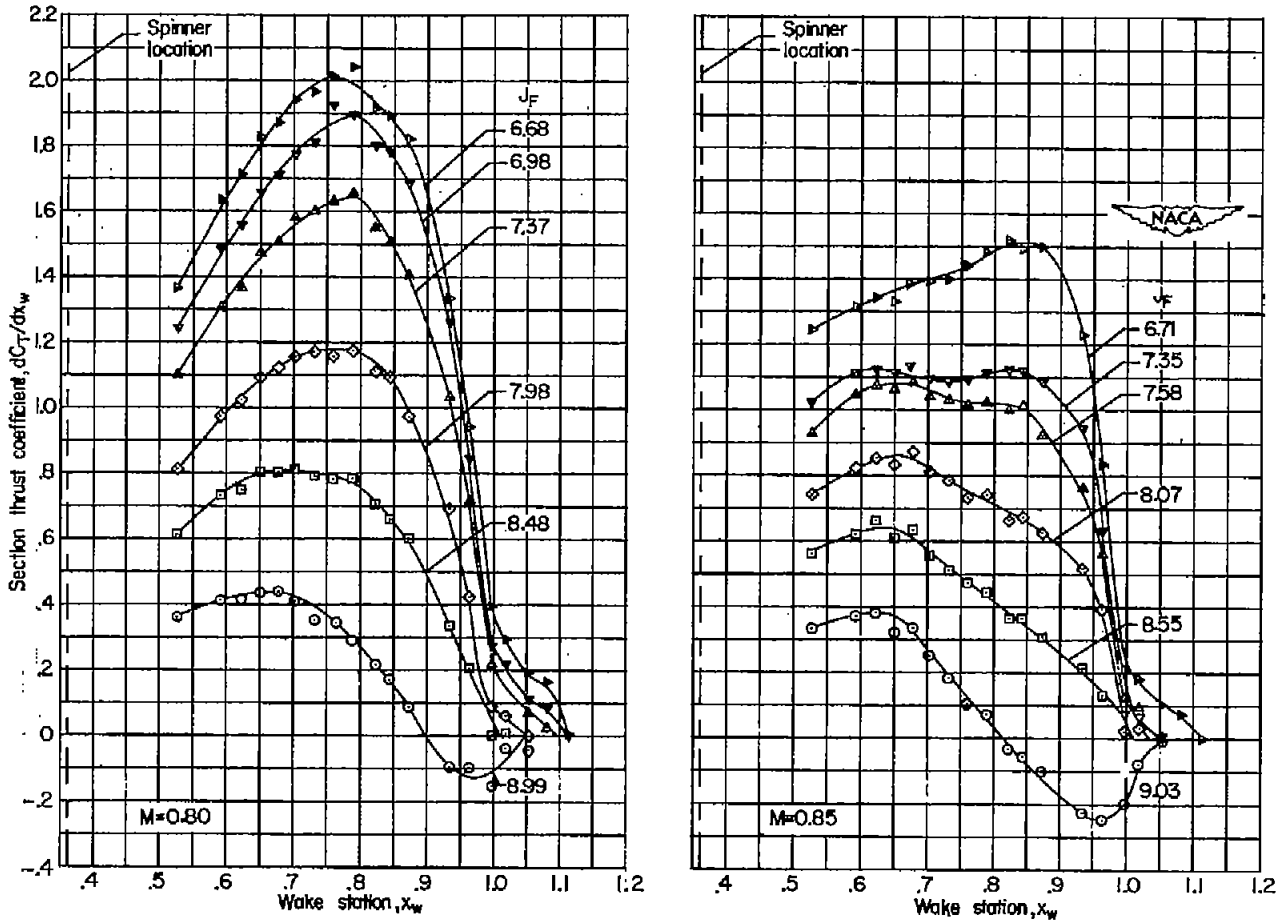

(e) M = 0.80 and 0.85.

Figure 7.- Continued.

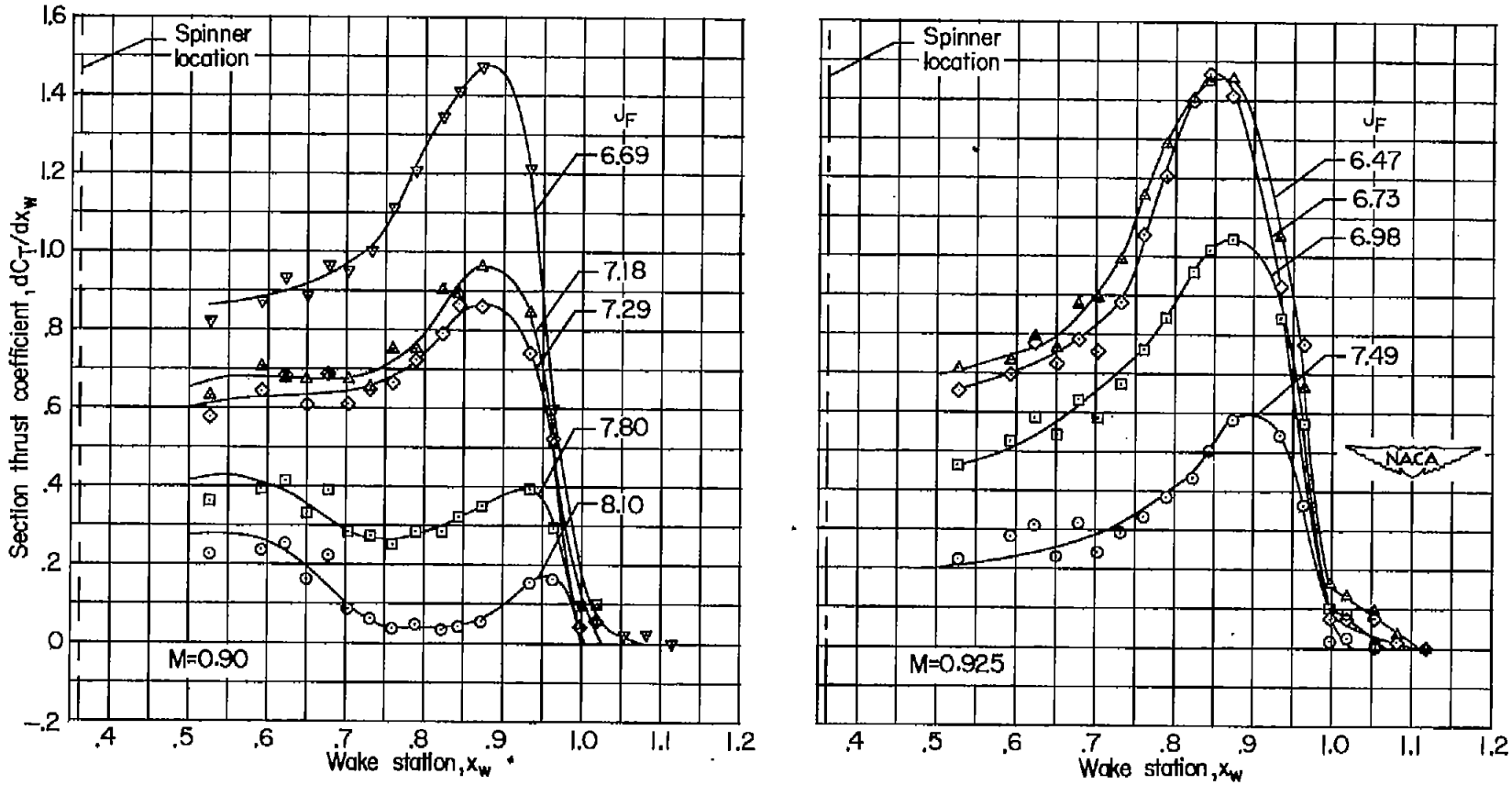

(f) M = 0.90 and 0.925.

Figure 7.- Concluded.

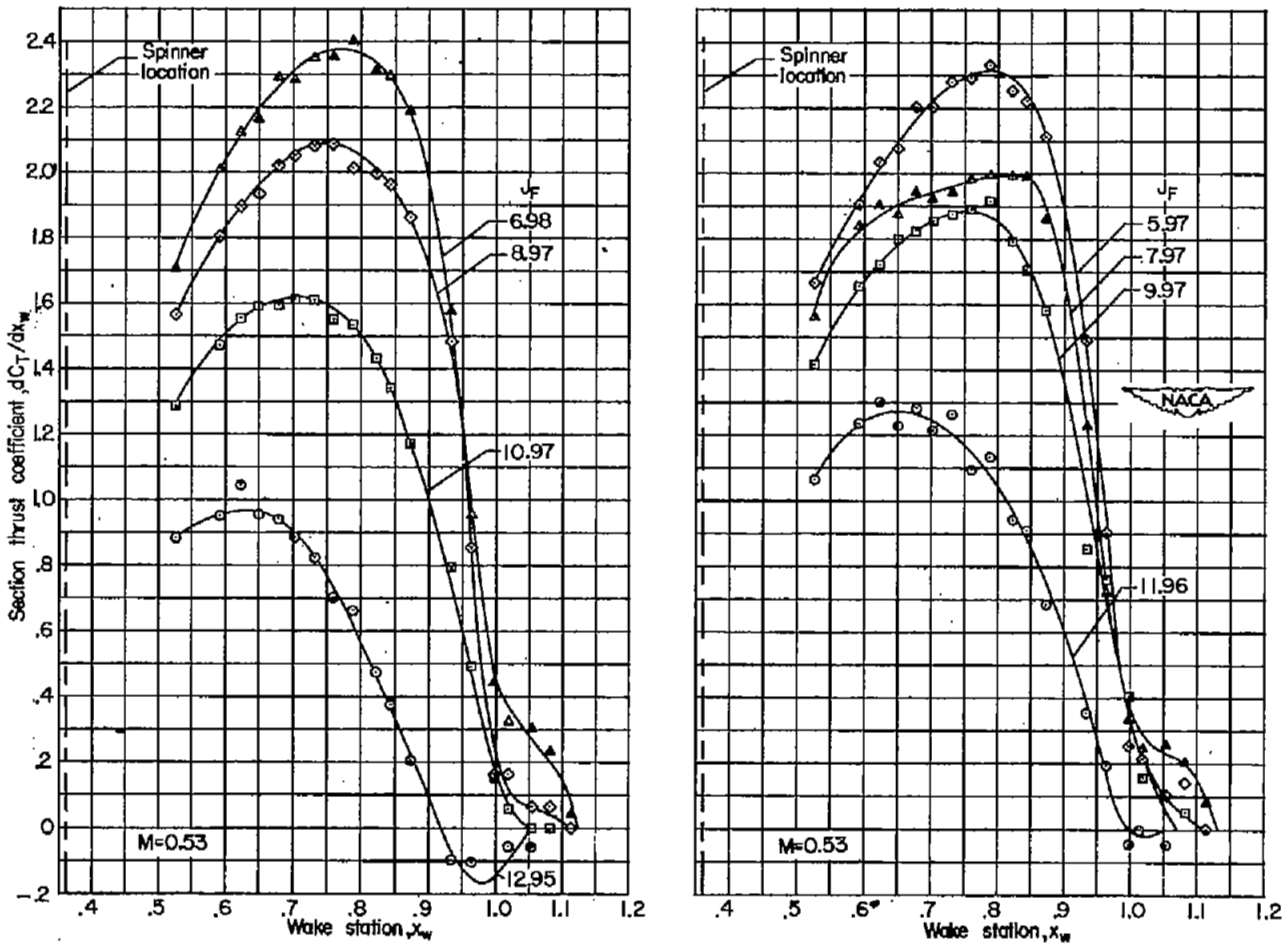

(a) M = 0.53.

Figure 8.- Section-thrust-coefficient curves for NACA 3-(3)(05)-05 eight-blade dual-rotating propeller. $\beta_{F_{0.75R}} = 80°$; $\beta_{R_{0.75R}} = 77.8°$.

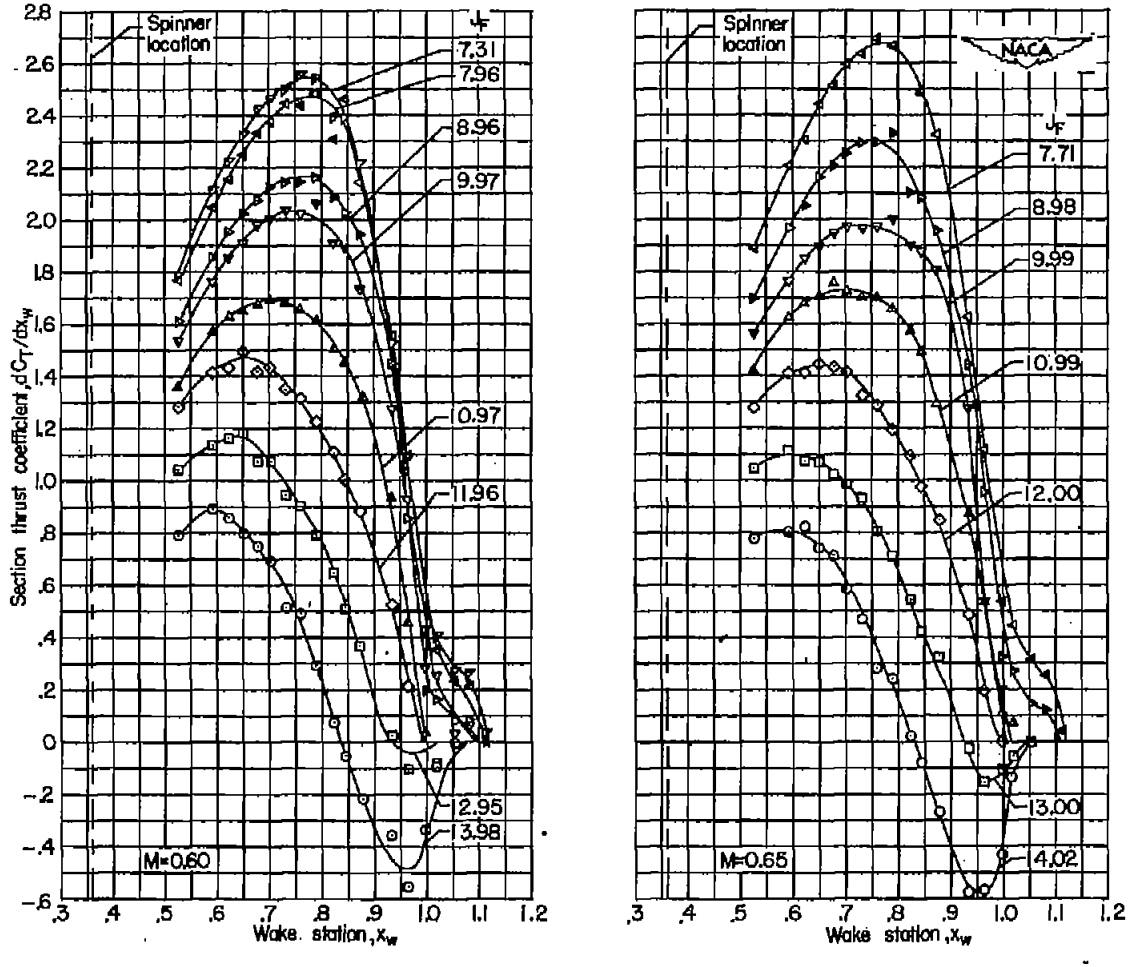

(b) M = 0.60 and 0.65.

Figure 8.- Continued.

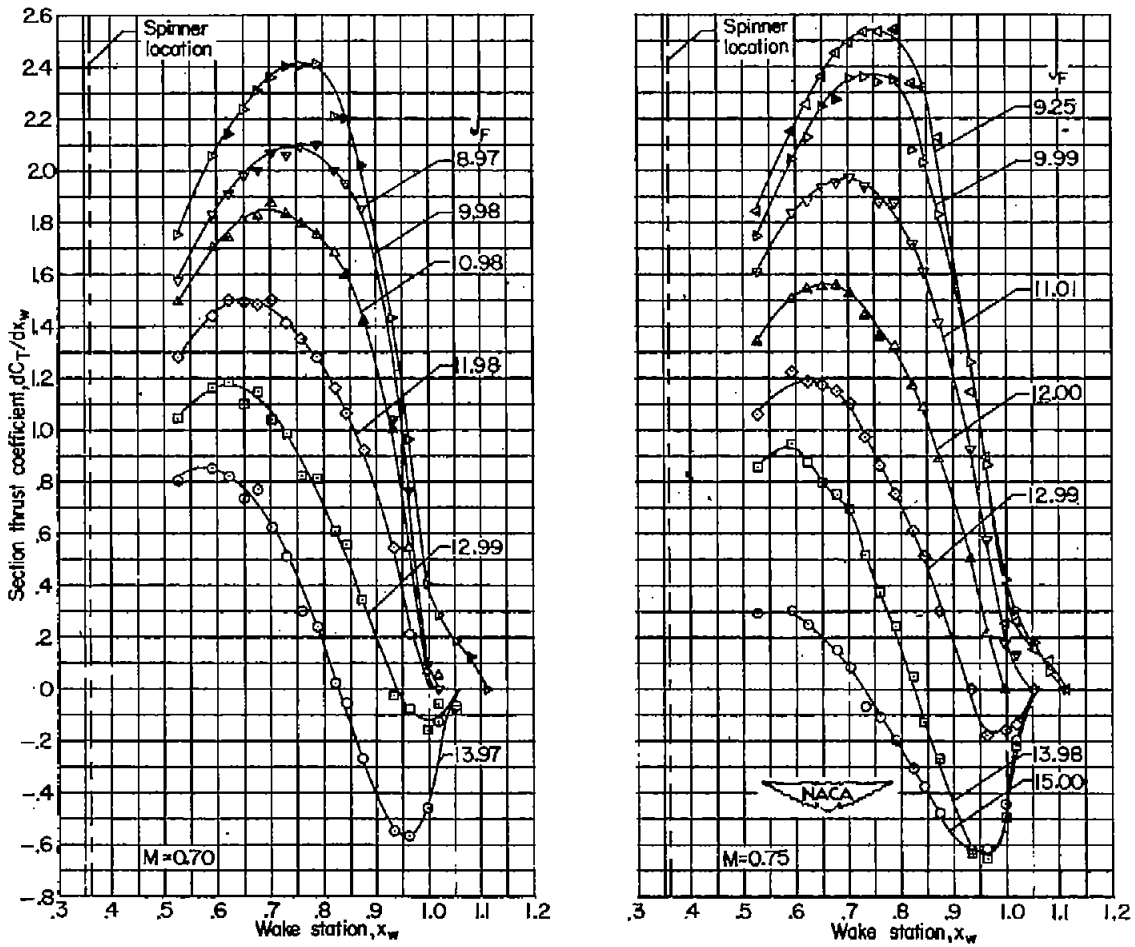

(c) M = 0.70 and 0.75.

Figure 8.- Continued.

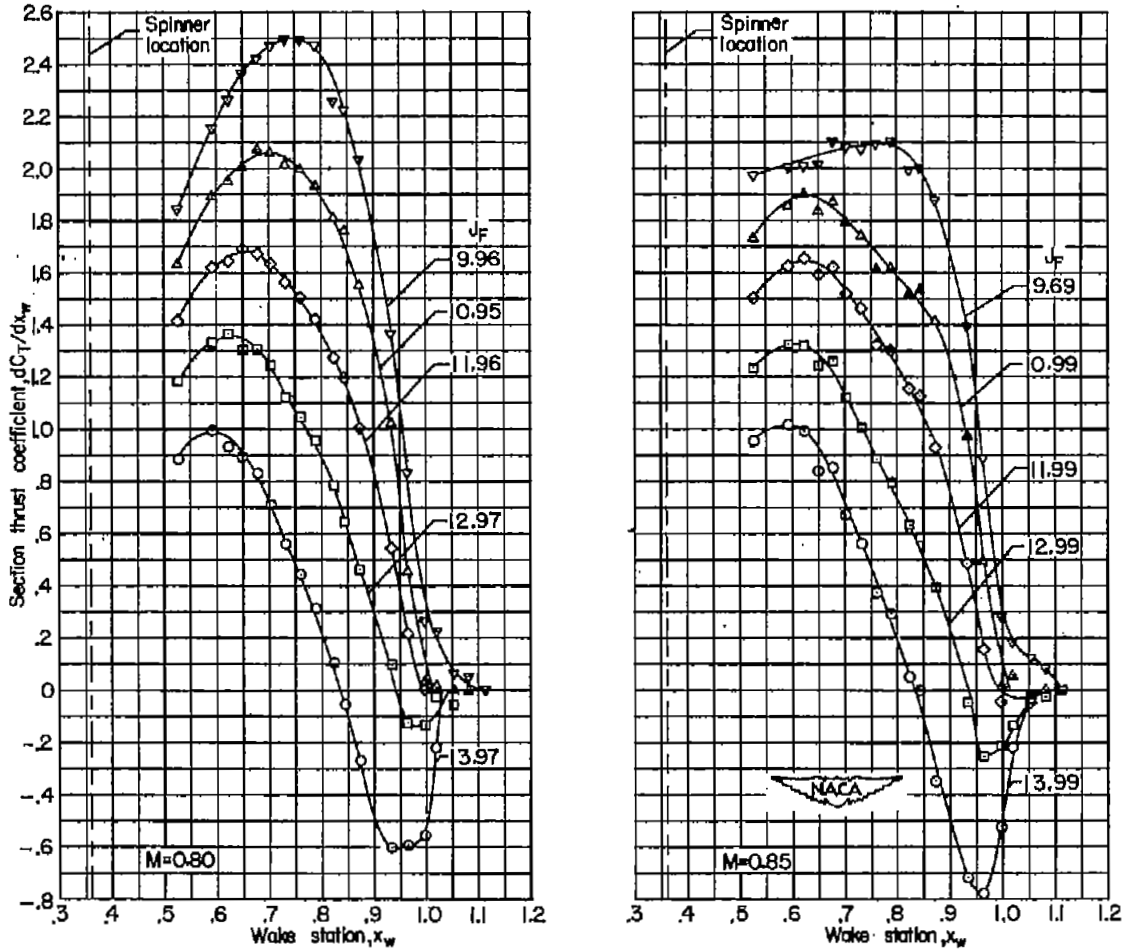

(d) M = 0.80 and 0.85.

Figure 8.- Continued.

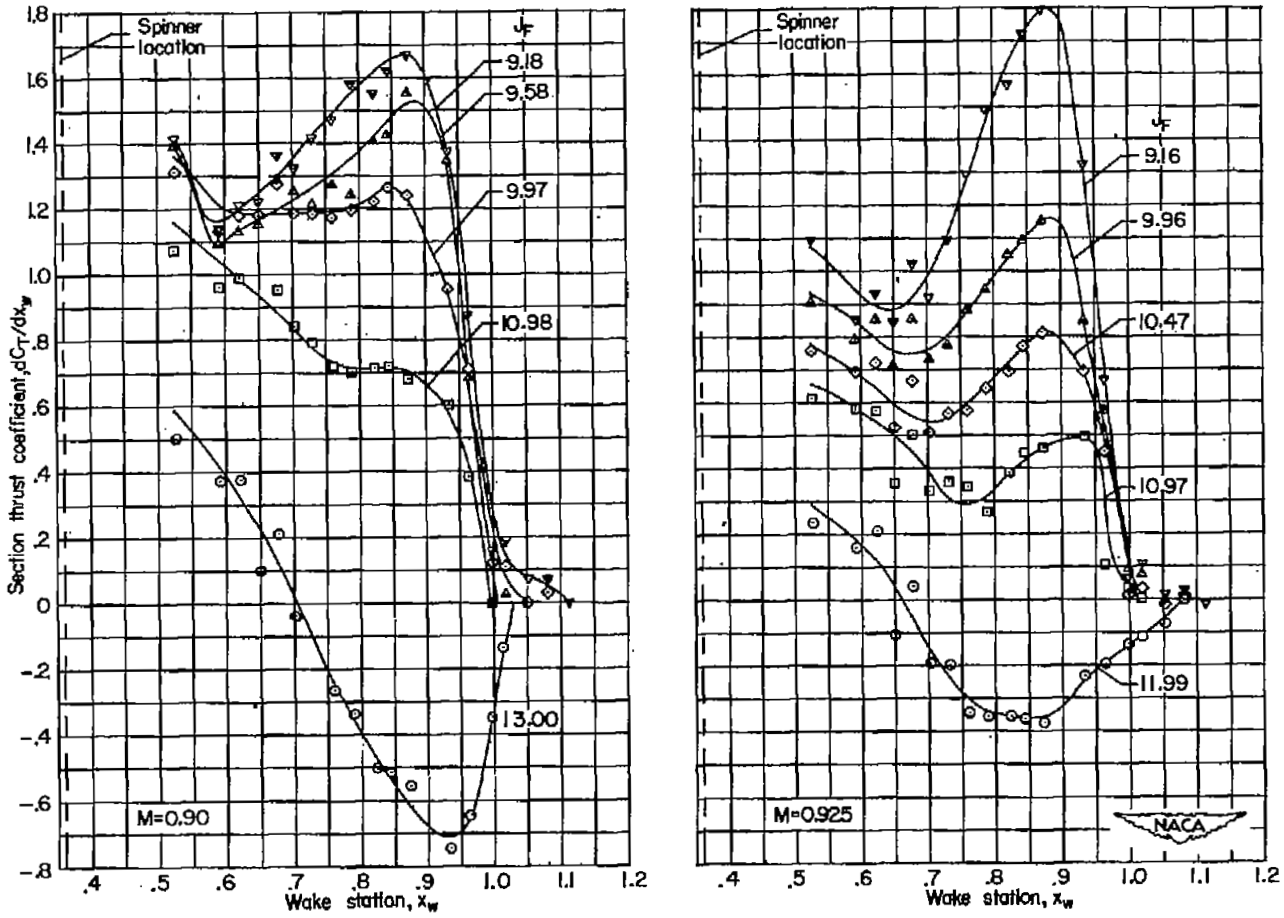

(e) M = 0.90 and 0.925.

Figure 8.- Concluded.

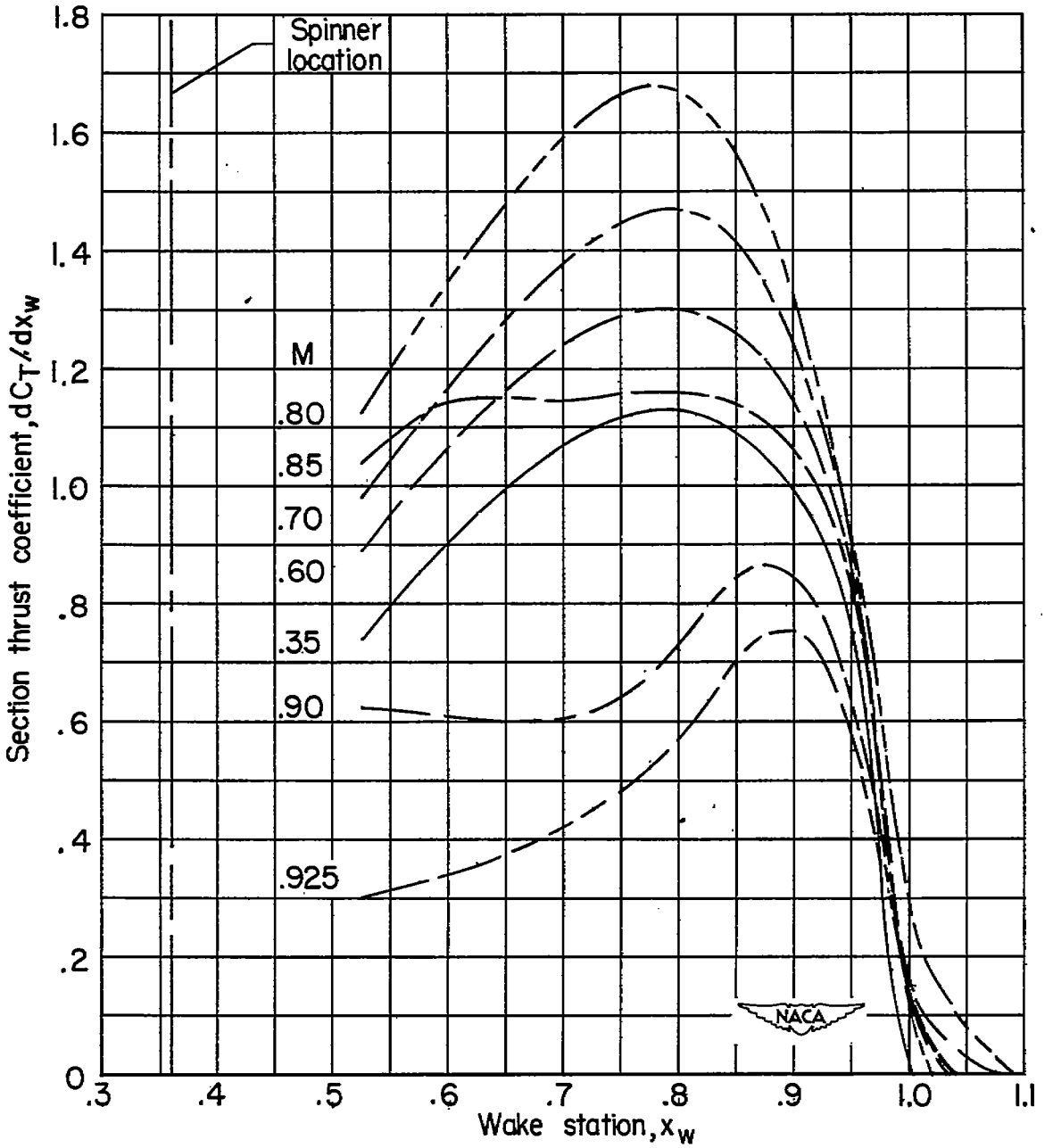

Figure 9.- Effect of forward Mach number on section thrust coefficient at constant advance ratio. $\beta_{F_{0.75R}} = 75°$; $\beta_{R_{0.75R}} = 73°$; $J_F = 7.3$.

[redacted]

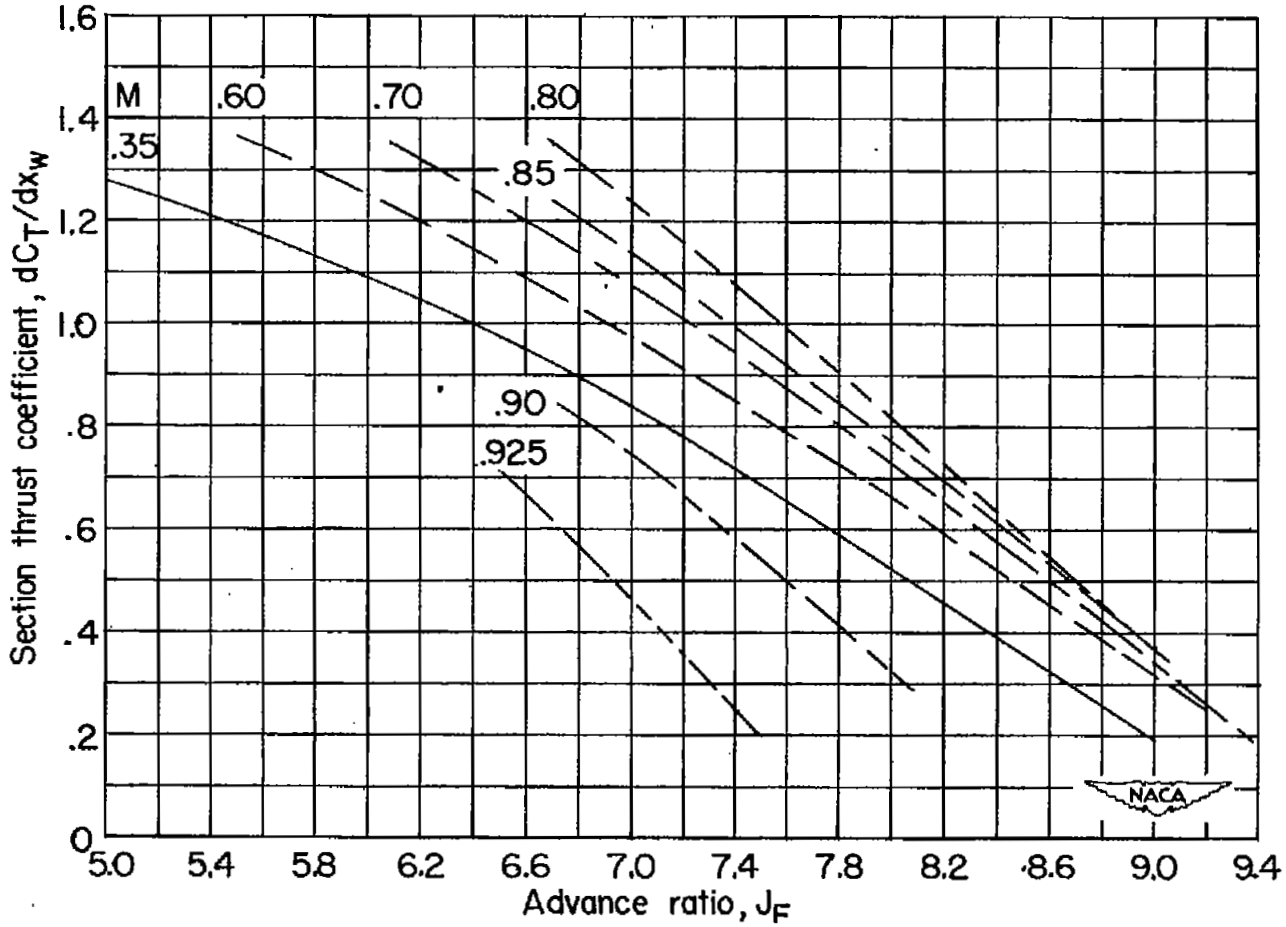

(a) $x_w = 0.525$.

Figure 10.- Variation of section thrust coefficient with advance ratio. $\beta_{F_{0.75R}} = 75^\circ$; $\beta_{R_{0.75R}} = 73^\circ$.

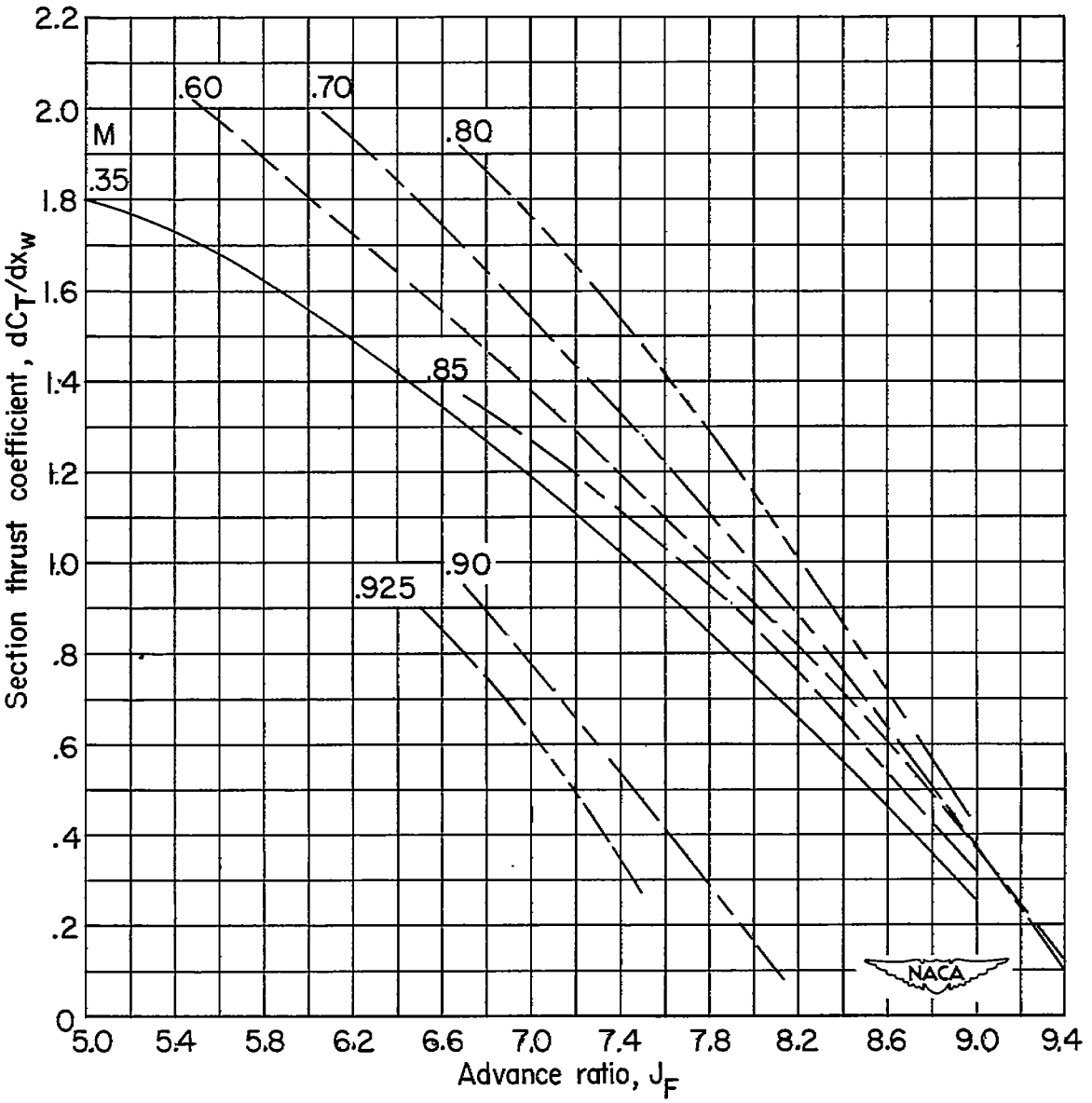

(b) $x_w = 0.70$.

Figure 10.- Continued.

[redacted]

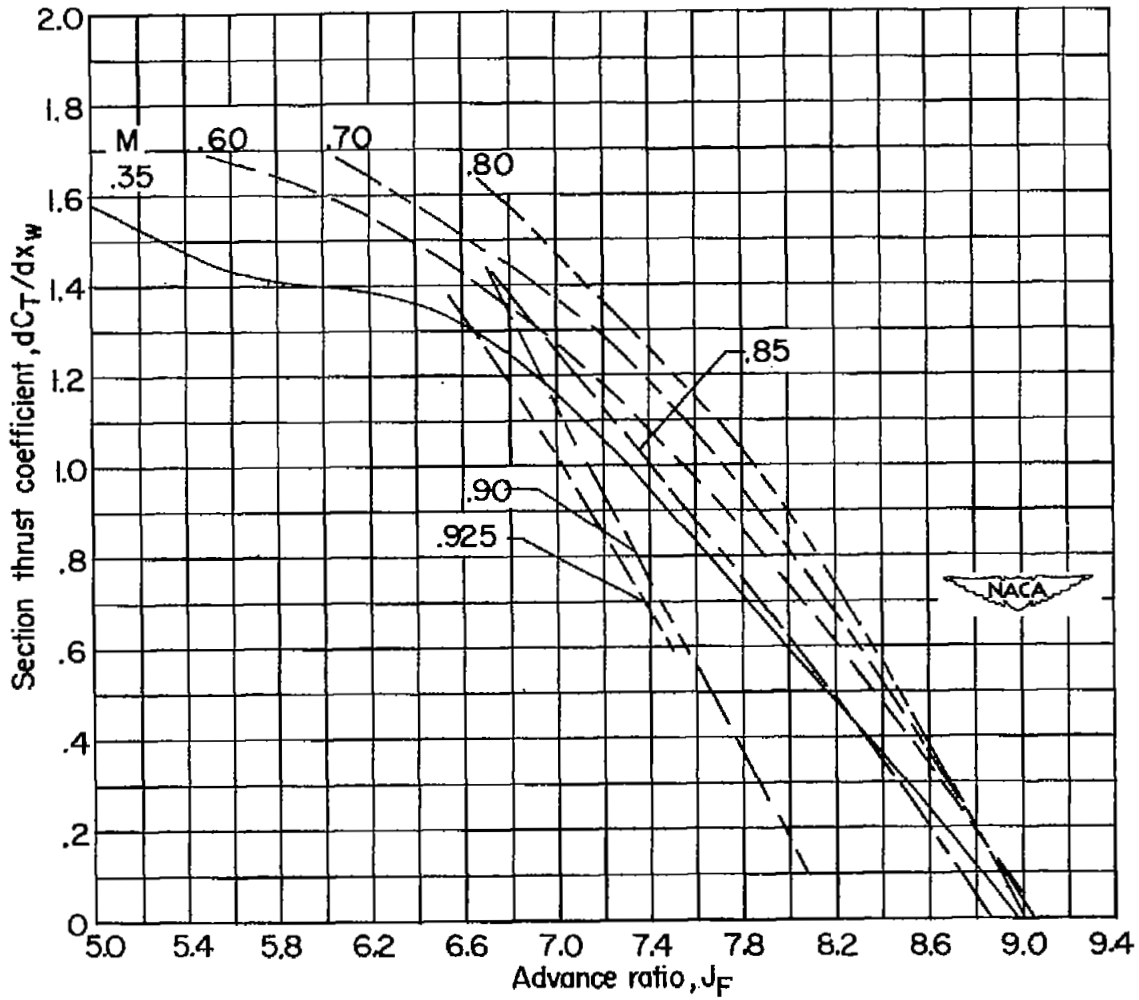

(c) $x_w = 0.90$.

Figure 10.- Concluded.

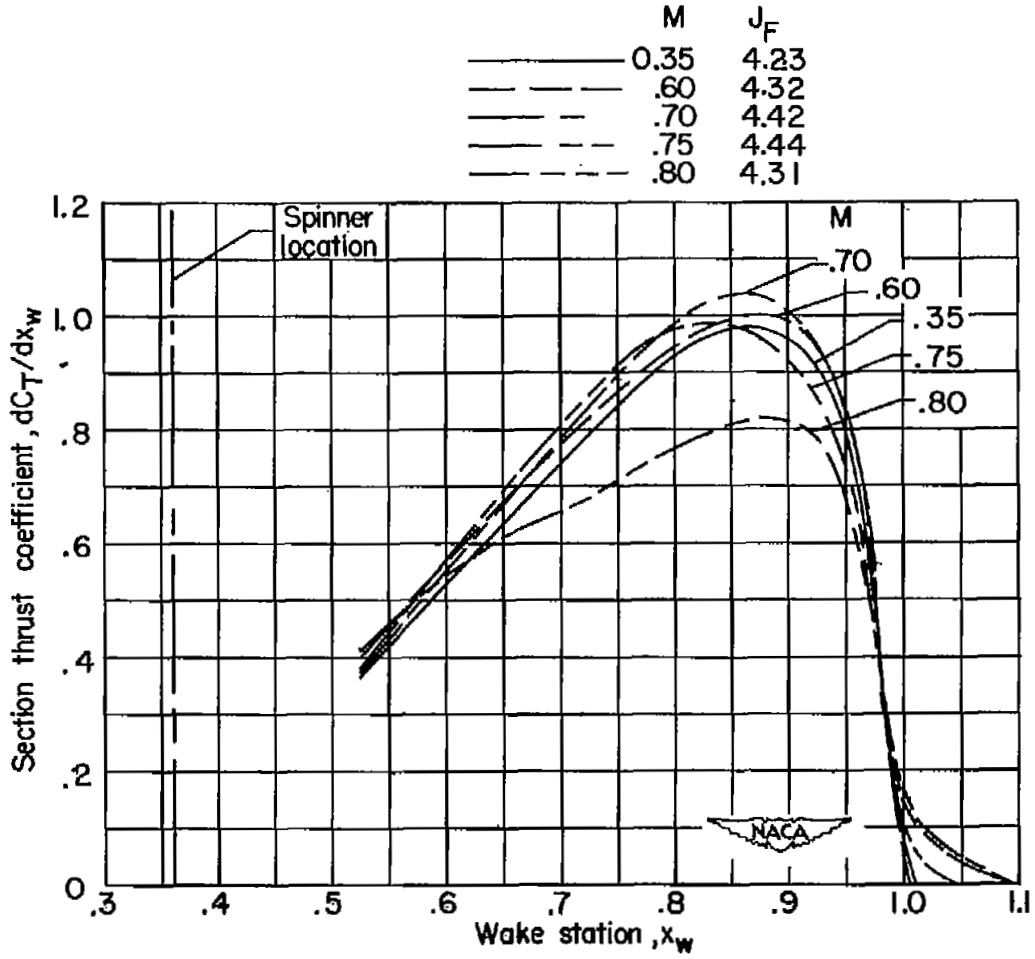

(a) $\beta_{F_{0.75R}} = 65^\circ$; $\beta_{R_{0.75R}} = 63.3^\circ$.

Figure 11.- Effect of forward Mach number on section thrust coefficient at maximum efficiency.

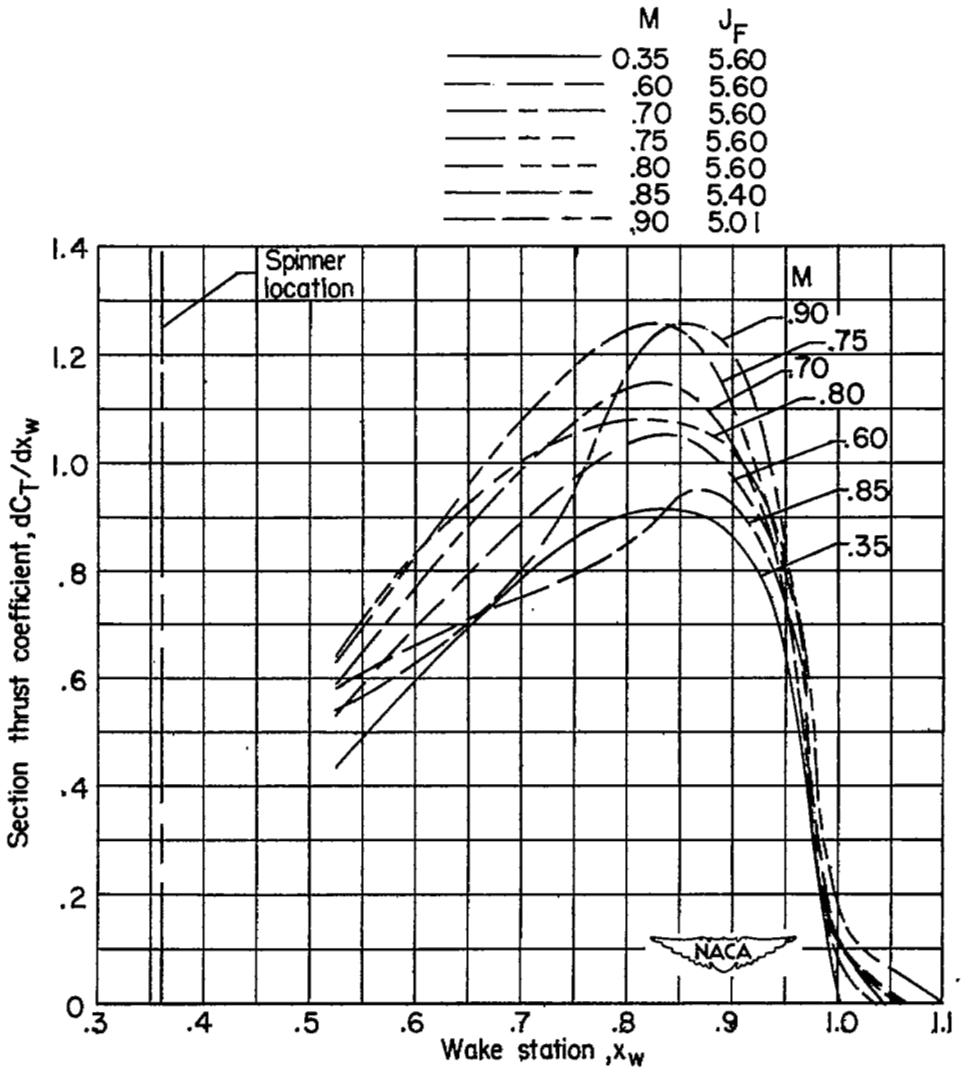

(b) $\beta_{F_{0.75R}} = 70^\circ$; $\beta_{R_{0.75R}} = 68.2^\circ$.

Figure 11.- Continued.

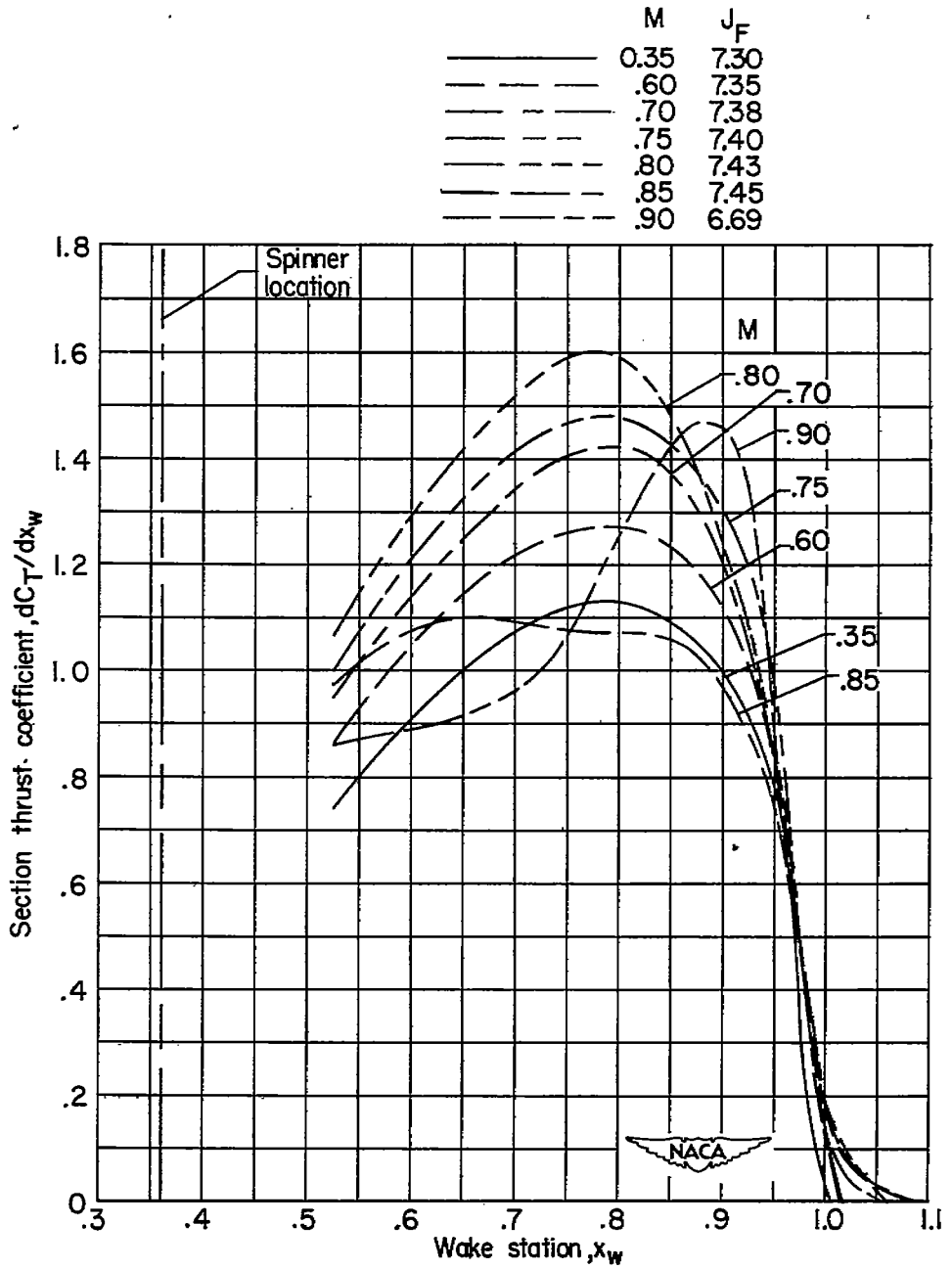

(c) $\beta_{F_{0.75R}} = 75^\circ$; $\beta_{R_{0.75R}} = 73^\circ$.

Figure 11.- Continued.

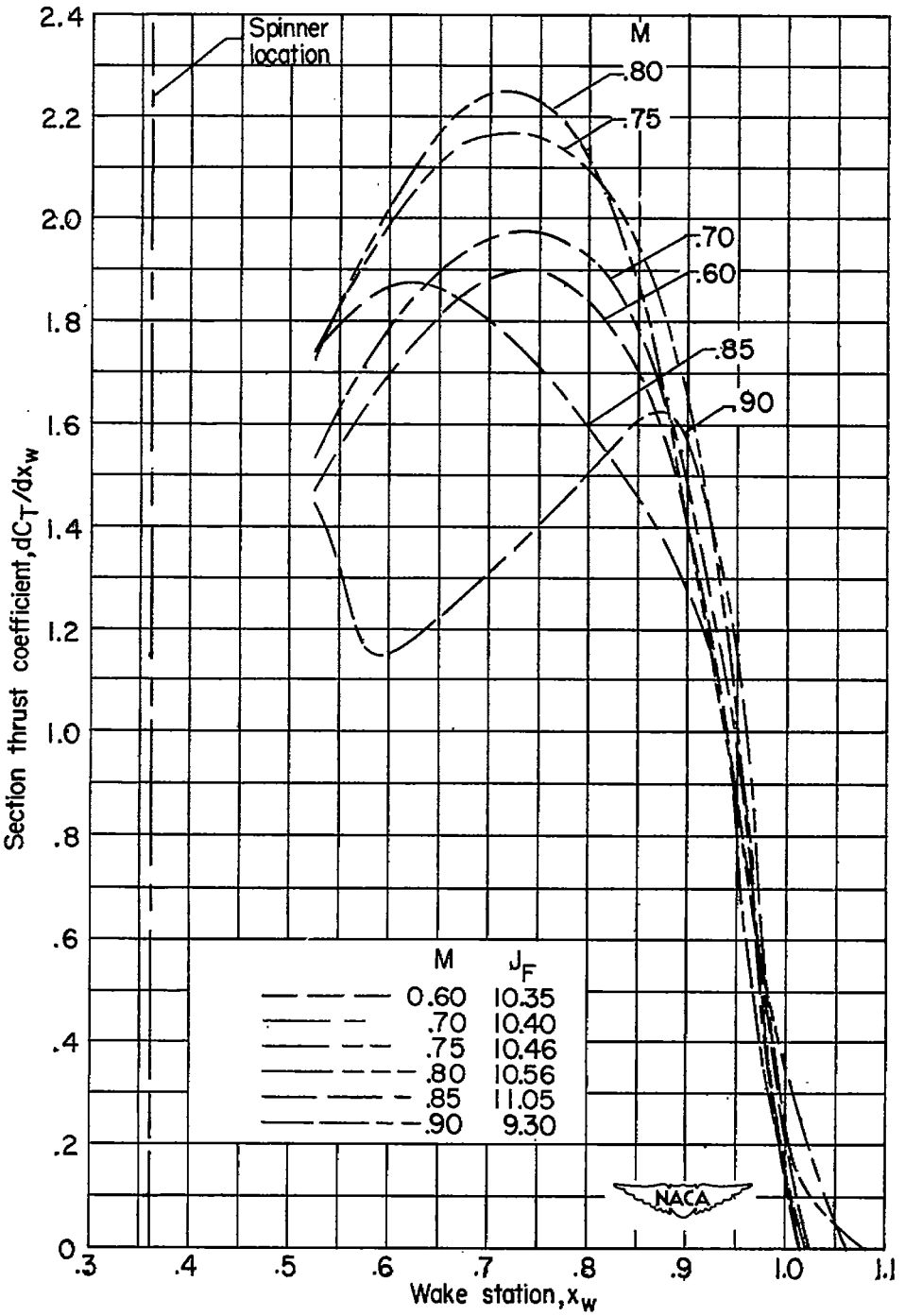

(d) $\beta_{F_{0.75R}} = 80^\circ$; $\beta_{R_{0.75R}} = 77.8^\circ$.

Figure 11.- Concluded.

NACA-Langley - 10-30-52 - 350

UNCLASSIFIED

UNCLASSIFIED